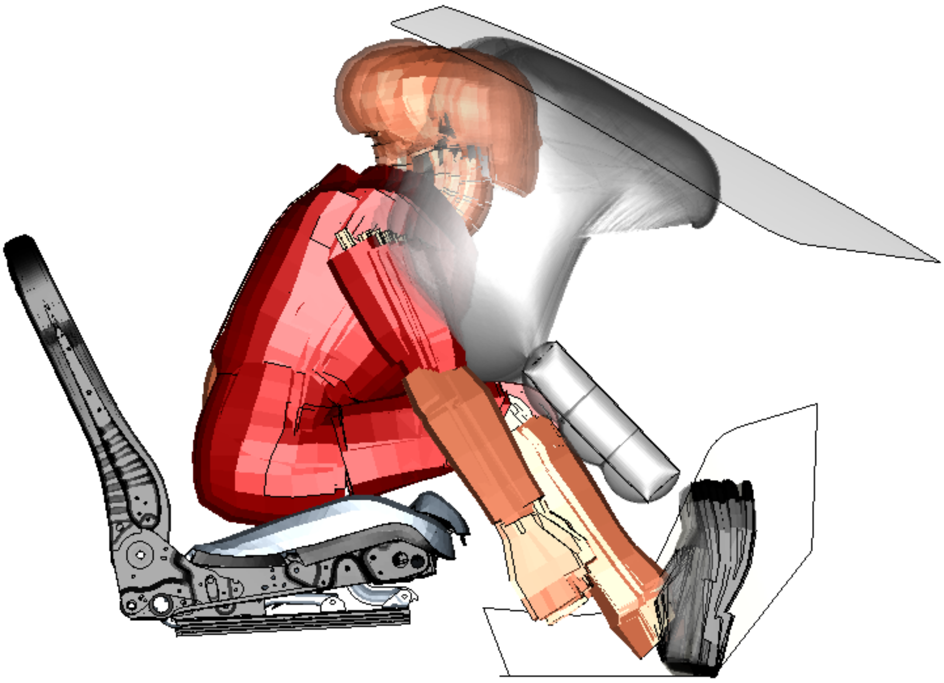

A Stochastic Approach for Parameter Relevance Estimation in Vehicle Interior Simulations of Frontal Impacts

Master's thesis in Applied Mechanics

WILLIAM HÜBINETTE

Department of Mechanics and Maritime Sciences
CHALMERS UNIVERSITY OF TECHNOLOGY
Gothenburg, Sweden 2019

Master's thesis 2019:67

A Stochastic Approach for Parameter Relevance Estimation in Vehicle Interior Simulations of Frontal Impacts

WILLIAM HÜBINETTE

CHALMERS
UNIVERSITY OF TECHNOLOGY

Department of Mechanics and Maritime Sciences
Division of Vehicle Safety
Chalmers University of Technology
Gothenburg, Sweden 2019

A Stochastic Approach for Parameter Relevance Estimation in Vehicle Interior Simulations of Frontal Impacts
WILLIAM HÜBINETTE

Supervisor: David Ramos, Volvo Car Corporation
Examiner: Johan Iraeus, Department of Mechanics and Maritime Sciences

Master's Thesis 2019:67
Department of Mechanics and Maritime Sciences
Division of Vehicle Safety
Chalmers University of Technology
SE-412 96 Gothenburg
Telephone +46 31 772 1000

Cover: Visualization of dummy position scatter in ten FE simulations of a frontal impact with varying input parameters.

Typeset in LaTeX
Printed by Chalmers Reproservice
Gothenburg, Sweden 2019

A Stochastic Approach for Parameter Relevance Estimation in Vehicle Interior Simulations of Frontal Impacts
William Hübinette
Department of Mechanics and Maritime Sciences
Chalmers University of Technology

Abstract

The evaluation of frontal crash performance of vehicles is mainly performed using standardized barrier tests and the safety system is designed against these. Innovation has led to improved technologies such as more accurate simulation models enabling us to improve how the safety system can work in a variety of scenarios. Thus, virtual crash tests using finite elements (FE) have almost replaced the physical tests among vehicle manufactures. The combination of faster computers and more accurate models has led to the possibility to simulate the variability in the system performance using stochastic simulations. If stochastic simulations are performed, which allows for testing of different design options and variability, information can be gathered as how to create a balanced and optimized safety system where all components work together at their best. In this thesis, simulations and physical tests of a currently used car platform are studied in full-frontal crash tests in order to determine which components need to be represented in the stochastic simulations. Based on the discovered behavior in theses tests, a list of relevant input and output parameters for the stochastic simulation is defined. Input parameters are sorted into three different types; production, design and real life, and both risk injury criteria and kinematics of a crash test dummy are used as output. Furthermore, a simplified and parameterized FE model of a vehicle interior for frontal impacts is developed and validated. Passenger airbag and knee airbag are simplified as unfolded airbags and a curve fitting function that measured the root mean square error between the reference airbag pressure and the simplified airbags is used to reproduce the behavior of the studied airbags. Floor and windscreen are modeled as rigid surfaces and the seat is simplified by removing parts of the backrest and prestensioned bolt connections are changed to rigid. The validation show that the simplified model deviates slightly compared to the studied tests, but it is approximately 14 times faster compared to the reference. Further, stochastic simulations are performed with geometrical, impact and airbag parameters varied. The statistical information such as mean, standard deviation and correlation between parameters is evaluated. The results produced from the simplified model follows the existing trends in the reference model making it possible to draw trend-based conclusions from the stochastic simulations. The stochastic simulations indicates that a crash pulse with low Vehicle Pulse Index is to strive for when developing a car to get low values of the risk indicators in full frontal impact. In general, the linear correlation matrix is a valuable tool to see the influence a variation of the input parameters have on the risk injury criteria and dummy kinematics. Lastly, different ways to present the data, i.e. scatter plots and history curves based on time data are visualized. In summary, the methodology developed offers an approach for using stochastic vehicle interior simulations in frontal impact, which can lead to a deeper understanding of the safety system and the opportunity to optimize and make it more robust.

Keywords: Stochastic simulation, Virtual crash testing, Robustness, Passenger airbag, Frontal impact, Finite element analysis, Passive safety

Acknowledgements

First of all, the project would not been possible without the help from my supervisor **David Ramos**. Thanks for all valuable advices and for always finding the time for discussions. Also a special thanks for not only acting as a great supervisor but also as a role model for me as a future engineer.

Secondly, I would like to thank **Emma Mårtensson** for making my time at Volvo Cars Torslanda pleasant and taking care of all the administrative work. Then I would like to thank all other colleagues at Volvo Cars for giving me a helping hand at any time needed.

Thirdly, all those people that have shared my pleasant time at Chalmers with me, including friends, professors and my family. For all love and support, thank you.

Lastly, thanks to my examiner **Johan Iraeus** who has showed great interest and support in my work.

William Hübinette, Gothenburg, June 2019

Nomenclature

All abbreviation occurring in the report are listed alphabetically in the table below.

ATD	Anthropocentric Test Device
AIS	Abbreviated Injury Scale
CAE	Computer Aided Engineering
CD	Chest Deflection
FE	Finite Element
FMVSS	Federal Motor Vehicle Safety Standard
HIC	Head Injury Criteria
HIII	Hybrid III
KNAB	Knee Airbag
LHS	Latin Hypercube Sampling
NCAP	New Car Assessment Program
PAB	Passenger Airbag
SDOF	Single Degree of Freedom
THOR	Test device for Human Occupant Restraint
VCC	Volvo Car Company
VPI	Vehicle Pulse Index

Contents

1 | Introduction

According to the World Health Organization, the number of road traffic deaths continues to rise steadily, reaching 1.35 million in 2016 [1]. As an example on how severe these numbers are, road traffic injuries are now the leading cause of death for young people aged between 5 to 29 years old. The majority of deaths occurs in low income countries, but accidents happens all over the world. The Insurance Institute for Highway Safety states that almost 24000 people were killed in car accidents during 2017 in the US [2]. Of all these deaths, more than half occurred in frontal impacts.

Modern cars are tested through several crash tests including frontal impacts before they are released on the market. Moreover, advanced restraint systems such as airbags and seat belts are used, and still fatal injuries occur in traffic. One of several causes to this is that real life crashes can show an infinite number of variation and it is hard to design a safe car for all types. To ensure that a car is safe, repeatable crash tests are done. However, the variation is also found in these [3]. It has been proven that the relationship between the commonly used Hybrid III crash test dummy and any injury risk is highly sensitive to experimental factors, e.g. test speed, restraint conditions and seating position [4]. Hence, not only the real life accidents vary, but also the tests used to design the restraints systems. This is a fact that every safety engineer works with every day and even if it would be easier to develop safe cars in a deterministic world, the true world is stochastic.

Evaluating variation in physical tests is costly and time consuming. An alternative to physical crash testing is virtual simulations with FE models of the complete vehicle. The automotive industry is one of the drivers of virtual product development since it is necessary to develop innovative, high quality cars within a short time. Furthermore, in order to speed up the process even further, the complete car simulation models used for crash testing can be simplified to generic and parameterized models consisting only of the most necessary components. The method is used in both development and in research, e.g. Iraeus et al. [5] and Deng et al. [6].

One of the intentions of speeding up the simulations is to be able to run stochastic analyses where hundreds or thousands simulations are performed to see the spread in results. The stochastic simulation is based on parameter variability. For one simulation, the input parameters are sampled from several distributions and a simulation is executed. The stochastic simulations can be used not only to understand how the safety components work by themselves, but to create a robust and optimized safety system which is not that affected by variation and where all components work together at their best.

1.1 Purpose

The aim of the Master's thesis is develop a method to investigate the parameters affecting the frontal passenger safety performance with focus on geometrical parameters of the interior and crash pulse, and how they affect the dummy injury criteria and kinematics in a full-frontal crash. The purpose of the investigation is to find statistical relationships in order to optimize the safety system performance. In the Master's thesis, a method to develop and validate a simplified vehicle FE model for frontal impact is also included. The model will make it possible to perform stochastic simulations in a relative short time. Furthermore, the purpose of the method is not only to get a simplified model, but also to investigate how components can be simplified and tuned.

1.2 Limitations

There are almost equally many women as men in the world and all humans' are in some sense have different antropometry. Despite this, the thesis will only take a 50th percentile male dummy into consideration since more data is available to validate the model against and the size of the dummy is between the smaller and larger dummy which makes it the best choice if only one dummy is used. Moreover, only one load case will be evaluated, i.e. the frontal impact with focus on an unbelted front seat passenger. The load case is without seat belt to reduce the complexity of the model and to focus more on kinematics which vary a lot more in a free flying unbelted load case.

A crash pulse from a frontal impact may cause the car to move both in Y and Z direction and the car can both pitch and yaw. However, the pulse in this study is limited to one degree of freedom only, i.e. the simplified model is only accelerated in the X direction and no rotation is applied. Moreover, only one impact speed is evaluated in the project.

The investigation of parameters affecting the safety performance is limited to geometrical parameters of the interior, e.g. instrument panel, seat and airbags. Moreover, only a few parameters are varied in order too keep the amount of simulations within a reasonable range.

To validate the performance of the simplified vehicle FE model the results from the simulations are compared to FE models of the current Volvo platform which are regarded as accurate. Parameter tuning is only performed once to increase the correlation between the simplified model and the reference model due to the time limitation.

1.3 Methodology

First, in order to understand the principles of stochastic simulations in vehicle safety, an overview of the existing literature was made. The review was focused on model simplifications, parameter distributions and related topics. Following the literature study, a few physical tests and simulations of unbelted frontal impacts performed by VCC were studied. The intentions with the study were to see which parts in the car the dummy interacts with and how a variation of these parts affects the dummy. This analysis of the variation is preliminary and a list of possible input parameters were defined as a result. Further, in order to see the kinematic effect from the input parameters, a script in the post-processor META was developed to extract the rotations and displacements of the dummy that were found interesting to study in a frontal impact.

A simplified model of a frontal passenger vehicle interior was developed and parameterized in the pre-processor ANSA. Parallel to this process, 28 generic crash pulses were defined with varying Vehicle Pulse Index (VPI) [7]. In connection to the model development, parameter tuning in LS-OPT was performed in order to get a better correlation between the simplified model and the more detailed model used as reference. In addition, all simplified components were tested in a test against its detailed replica to understand the level of validation and main sources to deviations in the simplification.

Furthermore, the stochastic simulations were performed with the parameter distributions decided by the engineers at VCC via LS-OPT. The data from the test were analyzed, processed and visualized using both META and the programming software MATLAB. Finally, comparison between the input and output were presented in correlation matrix, scatter plots and history curves based on time data and the results were discussed.

2 | Frame of reference

This Chapter will first present a literature overview of the specific area with focus on stochastic simulations connected to vehicle safety, and secondly explain some general theory regarding crash testing and simulations.

2.1 Literature overview, stochastic car crash simulations and dummy kinematics

Similar research has been performed by different academia and automotive manufactures. Hence, valuable information about both method development and which parameters influence the safety system can be gathered. To collect and examine the state of the current knowledge in the field, searches were done using a combination of different keywords such as "Occupant restraint system", "Finite Element", "Simulation", "Crash", "Stochastic analysis", "Probability", "Robustness evaluation", "Vehicle safety", "Parameter study", "Statistics" and "Generic car model". Results from manufactures and research articles were prioritized.

The number of studies found in the specific area of the current study was shown to be modest. Some studies were found where they perform stochastic and statistical analyzes of the vehicle restraint system, e.g. Deng et al. [6], Will and Baldauf [8] or Taewung and Hyun-Yong [9]. Most research was carried out in countries with automotive manufactures, e.g. Sweden, Germany or USA. Researchers attempted to evaluate the impact of input scatter on important result parameters. The review is mainly focused to see which methods have been used in the stochastic simulations, e.g. sampling methods, what parameters that are important for the injury outcome and model simplifications.

Researchers have attempted to evaluate the impact of varying different parameters in the passive vehicle safety system to identify how it will affect the injury criteria. Deng et al. [6] investigated the parametric effect of the side curtain airbag deployment interaction with the dummy in a side impact crash. The load case is different from the one used in this thesis, but many similarities exist, and conclusions can be used for frontal impact as well. First, the input parameters considered were the following: airbag-head separation distance, airbag trigger time, initial airbag inlet temperature, number of computational particles employed representing the amount of air in the airbag and moving barrier strike velocity. As output to the experiments, HIC36 and peak head acceleration were used. A total of 27 simulations were performed in a simplified vehicle environment with combined minimum, mean and maximum values for the input parameters. In conclusion, changing the input parameter led to a widespread in head acceleration, the most influential factors were the velocity of the impact barrier followed by the initial temperature in the airbag.

Further, Will and Baldauf [8] suggested a method to include scatter of important input variable of the restraint system and test conditions into the design process. The stochastic simulations were ran with scatter in airbag variables, friction variables, geometrical positions of dummy and impact pulse. The results gathered were mainly focused on injury criteria. In order to run several simulations in short time, a simplified vehicle model only consisting of the vehicle cockpit was used. The article highlights the importance of finding the correct statistical information of the input parameters. As a result, scatter plots and correlation between the input and output were presented and conclusions about necessary modifications of the restraint systems could be drawn.

Similar studies with simplified models have been done by Taewung and Hyun-Yong [9], and Avalle et al. [10]. Taewung and Hyun-Yong validated the head, chest and pelvis accelerations of a MADYMO model for frontal impacts. Further, they did stochastic analysis using the model and calculated the injury criteria sensitivity to different input parameters to find the most influential parameters. The mean and standard deviation of the crash pulse, mass flow rate of the inflator were calculated from test data and other input parameter were tuned with reversed engineering. Lastly, the mean of the injury criteria was reduced by designing the safety components based on an optimization procedure. Similar, Avalle et al. did stochastic analysis developed by using a generic car model. However, instead of changing parameters in the restraint system, structural parameters such as steel sheet properties were used as stochastic input variables. In general, methods and tools to visualize results from stochastic simulations were presented, e.g. histograms, linear and quadratic correlation matrices and correlation bi-plots.

In a more recent study by Iraeus [5], a parameterized FE generic driver vehicle buck model was created and validated against real life crashes. Stochastic simulations were ran with 27 varying input parameters including scatter in airbag parameters, geometry, friction, impact pulse and direction. The crash pulse shape and distribution were derived based on real life frontal crashes. The output in the simulations was the risk of rib fracture. The final model provides a possibility to develop and evaluate new passive safety systems for senior occupants based on real life crashes.

Overall, these studies highlight the need for model reduction in order to save CPU time and provide faster results suitable for stochastic simulations. However, the simplified model needs to be validated. They also pointed out the importance of finding the statistical distributions of the input parameters used in the simulations. Further, it is beneficial if the process of extracting output data is automated in order to reduce time on post-processing. Lastly, statistical measures such as correlation analysis or sensitivity analysis are tools used to draw conclusions.

Moreover, several authors have considered studying the dummy kinematics for both different load cases and dummy positions. Dongseok et al. [11] studied the influence of the restraint system in small overlap frontal impacts with the forward and outward head displacement as output. The study showed how it is possible to increase the restraint performance by looking at dummy kinematics. Further, Bastien et al. [12] measured angular changes of the head and chest of a dummy to see the effect on occupants' kinematics and injuries for neck, head and thorax in an emergency braking scenario, considering various occupants' driving postures. To sum up, these studies indicated on how dummy kinematics can be measured in a crash scenario to catch important movements, e.g. head and chest displacement and rotation.

2.2 Coordinate system in Volvo cars

In order to consistently refer to different directions and positions in the car, a global coordinate system has been defined. The X-direction is defined pointing from the front of the car to the rear, the Y-direction is defined from the drivers left hand side to the right and is defined as zero in the center line of the car. Lastly, the Z-direction points from the road level and upwards, see left figure in Figure 2.1. The orientation of the global coordinates is the same for all Volvo cars but the Z and X origin may change between models.

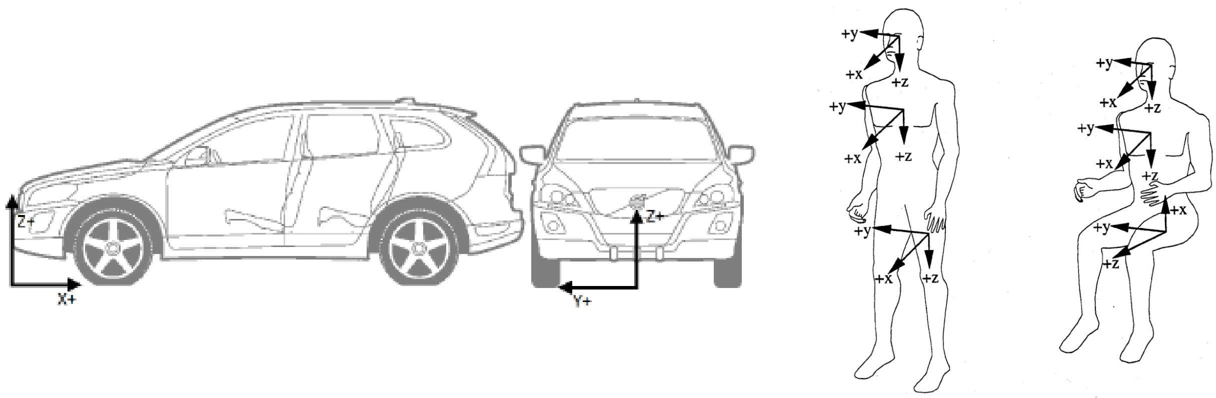

Figure 2.1: Illustration of global coordinate system used in a Volvo car (left), and coordinate system in dummies (right) [16].

2.3 Anthropocentric Test Devices

Anthropocentric test devices, or dummies, are used to evaluate how well the car and restraint system protects the occupant. They are mechanical surrogates of the human body used to estimate how effective the occupant restraint systems are in car designs. They are designed to imitate human physical characteristics, e.g. size, shape, mass, stiffness and energy absorption, such that the mechanical response in a specific crash scenario corresponds to the human response, i.e. trajectory, velocity, acceleration, deformation, and articulation. Further, the dummies are equipped with transducers and accelerometers to measure loading, deformation and accelerations of different parts. The data from the sensors can be compared to specific risk indicators or injury criteria to analyze the severity of the crash with the tested restraint system. Lastly, the dummies are classified according to their size, age, sex and impact direction such as frontal impact, side impact and rear impact [13].

The most commonly used dummies in frontal impact testing belongs to the Hybrid III family. The different sizes available represents a 3-year-old, 6-year-old, 10-year-old, 5th percentile female, 50th percentile male and a 95th percentile male. In automotive industry, the midsize adult male dummy is the most utilized size in restraint testing. The midsize adult male dummy represents the median height and weight of the 50th percentile adult male population [14]. Other dummies such as the THOR (Test device for Human Occupant Restraint) has also been developed for frontal impact. Compared to the Hybrid III, the THOR dummy has more instruments and has enhanced biofidelic features [15].

2.3.1 Sensor system in crash test dummies

The dummies are instrumented with sensors that measure accelerations, forces, moments, angular velocities and deformation of different body parts. The exact set of sensors is varying between different dummy types. The coordinate system in a dummy can be seen in the right figure in Figure 2.1, note that the local coordinate system for each body part moves with the limb they belong to with the positive z-direction pointing towards the distal end. Acceleration is measured in G which is not a SI-unit. Forces are measured in SI-unit Newton and forces in X and Y direction are shear forces in the sagittal and frontal plane, and the Z-forces are tension-compression forces. Moments are measured around it specified coordinate axis, e.g. M_y is the moment around the Y-axis and is measured in SI-unit Newton per meter. Lastly, the deformation is measured in millimeter [16].

2.4 Safety rating, legal and consumer based crash tests

In today's car industry, safety rating has a large role to play. Several organizations evaluate the safety of cars. The New Car Assessment Program (NCAP) aims to improve occupant safety by implementing comparative safety tests making it possible for customers to make a choice regarding the safety of the cars. It also aims to encourage car manufactures to improve the safety of their vehicles. The program has developed standardized tests used to determine the safety rating of the car. The vehicles are assigned star rating for their performance in e.g. frontal, side and rollover crash testing, and the performance score is calculated from measurements obtained from dummy instruments. An example of a test in Euro NCAP is the full width rigid barrier test. Cars are tested against a rigid barrier at a test speed of 50 kilometers per hour. A small female frontal impact dummy is seated in the front driver's seat and in the rear passenger side seat. In the end, after combining all load cases applicable to that NCAP, e.g. frontal impact, side impact, active safety etc., a safety rating of the car is computed where five stars is the highest rating [17].

Moreover, it also exists legal requirements, e.g. the Federal Motor Vehicle Safety Standard (FMVSS) 208 which is a standard for Occupant Crash Protection in the United States. These regulations are developed by The National Highway Traffic Safety Administration and all vehicles that are sold in the United States have to meet them. The standard contains different dimensional load cases compared to NCAP, for example unbelted load cases similar to the one used in this thesis [18].

For VCC, it is important to assure a high rating from these organizations. Hence, the car is in a certain extend dimensioned by these tests. In the design phase of a car, Volvo combines all legal, rating and insurance rating and add real life scenarios. On top of that it adds margin to ensure the 5 star rating as the safety system is not robust. The test evaluating the front seat occupant safety for this thesis is similar to the FMVSS208 full width frontal load case, see Figure 2.2. In the full width frontal impact test, the car is frontally crashed against a rigid barrier with an initial velocity of 40 kilometer per hour. Unique with this load case is the fact that the dummies are unbelted.

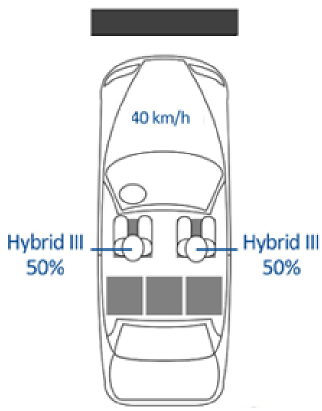

Figure 2.2: Illustration of full width frontal (unbelted 50th) load case in FMVSS208.

2.4.1 Injury Criteria

Injury criteria, or risk indicators, have been developed to couple the mechanical response from a dummy to injury risk for humans. The different injury criteria consist of risk curves which relates one value to the probability for an injury in that specific body region. Furthermore, the severity of the injuries are described by the Abbreviated Injury Scale (AIS) where the injuries are grouped based on how life-threatening they are, 1 is minor injury and 6 is severe injury. It is difficult to define the tolerance levels and risk curves since every human differs from each other. To establish the criteria used today, simulations, tests with cadaver, animals and human volunteers test below injury levels are methods that has been used [19].

One common way to measure the injury risk is by using the acceleration of different body parts. For instance, Head Injury Criteria (HIC) is estimating the risk of skull fracture and is computed with help of the acceleration measured in the center of the head. The value is calculated as shown in Equation (2.1) where $a(t)$ is the resultant acceleration and t_1 and t_2 are limits of the time interval that have the highest mean acceleration. The time interval can be either 15 milliseconds wide, or 36 milliseconds depending on which type of HIC used [20].

$$HIC = \max_{t_1,t_2} \Big\{ \Big[\frac{1}{t_2 - t_1} \int_{t_1}^{t_2} a(t)dt \Big]^{2.5} (t_2 - t_1) \Big\} \tag{2.1}$$

Moreover, the head, chest and pelvis maximum accelerations may also be used as risk indicators. It is common to use a 3-millisecond clip value extracted from the dummy. In the thesis, it is referred to as clip3m and is the maximum acceleration over an interval of 3 milliseconds. Other criteria commonly used are maximum Chest deflection, Neck Injury Criteria, Femur forces etc [20].

2.5 Vehicle restraint system

The restraint system of the car has a large influence on crash safety. The main components of the occupant restraint system for frontal impacts are the airbags and seat belt and their purpose are to restrain the occupant during an accident. During the impact, occupants will continue moving at the pre-impact direction and speed. Hence, the restraints system aims to slow the occupant over the longest time possible and distribute the forces over the largest possible area and to the strongest body parts. In this thesis, the belt will not be discussed since the focus is an unbelted load case.

2.5.1 Airbags in modern cars

There can be several types of airbags in a modern car, e.g. Driver airbag, Knee airbag (KNAB), Passenger airbag (PAB), Side airbag, Far side airbag, Curtain airbag, pedestrian airbag. In this thesis, a full-frontal impact will be evaluated for the frontal passenger side, hence, only KNAB and PAB will be used. Overall, the airbags work the same, the bag and an inflator is placed in an airbag housing. In a crash, an ignite in the inflator starts a chemical reaction which produces a gas that is pumped into the airbag which is built out of woven fabric. The time it takes to fully inflate the airbag varies but it is less than 1/20th of a second. The airbag is unfolded and pressurized such that it is positioned in front of the occupant. Straps are used to shape the bag and to keep it into position. Lastly, passive and active ventilation holes exist to establish the wanted pressure at the wanted time.

2.6 Crash testing with Computer Aided Engineering

Car crash simulations are a valuable tool for all car manufactures since the engineers can predict the outcome of a car design before it has been manufactured. This section will consist of the different features in a crash simulation and a short introduction to the different software used in this thesis to simulate a car crash, i.e. the pre-processor ANSA version 19.1.0 (BETA CAE Systems, Switzerland), FE-solver LS-DYNA (LSTC, Livermore, CA), optimization software LS-OPT (LSTC, Livermore, CA), and lastly the post-processor META version 19.1.0 (BETA CAE Systems, Switzerland).

2.6.1 Aspect of a car crash simulation

Many finite element models have been developed at VCC to study the impact of a car crash. During a crash simulation, large forces occur under a short period of time causing several non-linear phenomena to occur, e.g. material yielding and material breakage. Further, large deformation leads to geometrical non-linearities and different parts getting into contact with each other or even self-contact.

The non-linearities gives rise to the need of advanced and costly simulation models. VCC aims for high accuracy in the models while still making them as efficient as possible. Hence, certain guidelines for mesh size, element type etc. have been developed during the years to keep improving the quality. Further, continuous verifications of the model is made to ensure that it correlates to the physical product.

Car model
A complete FE model of a car consists of more than 10 million finite elements and a crash simulation takes more than 24 hours to simulate while running on 480 cores. Thus, depending on what is investigated, different parts are removed or modeled with less detail. As an example, one way to simplify an FE model for front seat crash safety evaluation is to model it without back seat or detailed luggage space. Further, not all simulations are performed with the car driven into something. It is common to apply the deceleration to a rigid boundary of the car or map the deformations to the cockpit from a complete vehicle simulation. For frontal impacts it has been the method of choice for all car manufactures since the beginning of virtual development. It works well since most of the deformation is taken by the front structure. Further, modern Volvo cars are built with a safety cage around the occupants made of high strength steel which makes the method work even better since less compartment intrusions exists.

Anthropometric test device
Every Hybrid III dummy is modeled as a highly detailed and validated FE model where the different body parts and joints have been introduced to correspond to the dummy used in physical testing. Each body part is modeled with solid or shell elements with material models corresponding to the material on the physical dummy. Instruments are located at the same position as the physical dummy. Acceleration is measured in different nodes and forces and moments are measured with FE beams and springs. The joints and self-contact are included to be able to capture the right kinematics.

Before every new crash simulation, the dummy needs to be positioned in the seat in an accurate way similar to when the physical crash test dummy is placed in the seat. In the preprocessing stage, the dummy is simulated down in the seat which will deform during the weight of the dummy. Hence, a contact force between the contracted foam of the seat and dummy occurs. The deformation and stress that occurs in the seat since it gets deformed can then be saved and used as an initial condition in further simulations. Thus, this only needs to be performed once for every combination of the dummy and seat position.

Furthermore, more simplified dummies can be used in simulations. One example is the Hybrid III FAST50 which is computationally inexpensive due to their low number of elements compared to the original Hybrid III 50th percentile dummy model. These dummies are also equipped with less instruments compared to other dummy models [21]. A comparison between the FE model Hybrid III FAST50, FE model of the original Hybrid III 50th percentile male dummy and the physical 50th percentile dummy is presented in Figure 2.3.

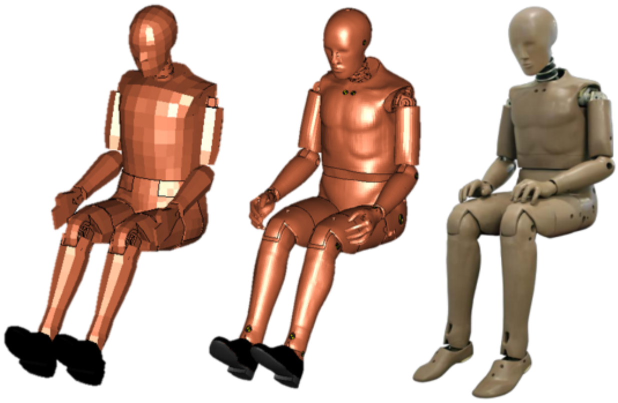

Figure 2.3: Comparison of FE model of the Hybrid III FAST50 dummy (left), Hybrid III 50th male dummy (center) and the physical model (right).

Airbag model

The airbag FE model consists of the same parts as the physical component, i.e. inflator, cushion and a housing, Figure 2.4 is showing the parts of an FE model of a passenger airbag (PAB). The FE models are delivered from suppliers with tunable parameters such as airbag ventilation hole diameter or trigger time. Furthermore, different methods of modelling the airbag are available in LS-DYNA but only one is used at the time. The most common used at VCC is either the hybrid or particle methods.

The hybrid model is based on control volume assumptions and results in an uniform pressure distribution in the bag. This method is relatively fast and robust but not that accurate if the area of interest is before the airbag is fully positioned, e.g. study deployment or out of position. The particle model is based on kinetic molecular theory where the many molecules in the air in the airbag is modeled as fewer particles. For each particle, a balance exists between the translation kinetic energy and the vibration energy when the particles collide with each other and with the fabric cushion. This method is more computational costly compared to the hybrid model, but it is more accurate in the airbag deployment phase. Hence, which model to use depends on the specific analysis [22, 23].

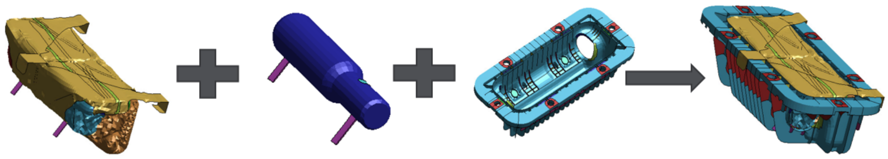

Figure 2.4: FE model of cushion, inflator and housing of a PAB.

2.6.2 Used software

LS-DYNA.
LS-DYNA is a FE solver with the possibility to solve highly non-linear transient dynamic FE problems. The solver has special entities available to model common car safety features such as belts with retractors and pre-tensioners, airbags and inflators etc. Further, the solver is command line driven. These command lines are often generated by pre-processor able to output the LS-DYNA run file as an ASCII text file [24].

The solver uses an explicit time integration method to solve the nonlinear dynamic problems. More specific, the explicit solver uses a time marching scheme called Central Differences to solve the system of non-linear ordinary differential equations. The time marching scheme writes the dynamic equilibrium at time n which allows the evaluation of the mid-step acceleration, then velocity and consecutively the displacements. The discrete dynamic equilibrium can be written as in Equation (2.2) where $\boldsymbol{M}$ and $\boldsymbol{D}$ are the diagonal mass and damping matrices, $\boldsymbol{f}^{int}(\boldsymbol{u})$ and $\boldsymbol{f}^{ext}$ are nodal vectors of internal and external forces, and lastly $\ddot{\boldsymbol{u}}$, $\dot{\boldsymbol{u}}$ and $\boldsymbol{u}$ are acceleration, velocities and displacement respectively [25, 26].

$$\boldsymbol{M}\ddot{\boldsymbol{u}}_h(t) + \boldsymbol{D}\dot{\boldsymbol{u}}_h(t) + \boldsymbol{f}^{int}(\boldsymbol{u}_h, t) = \boldsymbol{f}^{ext}(t) \tag{2.2}$$

The critical time step Δt_{cr} is computed by Equation (2.3) where l^e_{min} is the characteristic minimum element length, E is the Young's modulus and ρ the material density.

$$\Delta t_{cr} \leq \frac{l^e_{min}}{c^e} \ , \qquad c = \sqrt{\frac{E}{\rho}} \tag{2.3}$$

Assuming that the time-step is computed, application of the Central Differences to Equation (2.2) then leads to the following procedure:

- Calculate the acceleration $\ddot{\boldsymbol{u}}_n = \frac{\dot{\boldsymbol{u}}^{n+\frac{1}{2}} - \dot{\boldsymbol{u}}^{n-\frac{1}{2}}}{\Delta t_{cr}}$
- Evaluate the internal and external forces
- Calculate the middle step velocity by solving
  $\dot{\boldsymbol{u}}_{n+\frac{1}{2}} = [2\boldsymbol{M} + \Delta t\boldsymbol{D}]^{-1}[(2\boldsymbol{M} - \Delta t\boldsymbol{D})\dot{\boldsymbol{u}}^{n-\frac{1}{2}} + 2\Delta t(\boldsymbol{f}^{ext}_n - \boldsymbol{f}^{int}_n(\boldsymbol{u}_n))]]$
- Calculate the end-of-step displacements as $\boldsymbol{u}^{n+\frac{1}{2}} = \boldsymbol{u}_n + \Delta t\dot{\boldsymbol{u}}^{n+\frac{1}{2}}$

The computations are straight forward since the matrices $\boldsymbol{M}$ and $\boldsymbol{D}$ become diagonal as lumped mass matrix is used. The method is conditional stable but avoids several convergence problems. The stability is achieved by choosing a proper time-step as defined above. In other words, it means that the time-step must be smaller than the the time it takes for a sound wave to travel through an element. Further, this small time step suits crash analysis and high speed impact simulations well. In summary, the explicit solver in LS-DYNA using Central Difference is a trusted and good choice for running crash simulations.

LS-OPT.
LS-OPT is a graphical optimization tool that interfaces together with LS-DYNA. The software has a graphical interface where the user can structure design process, design space and compute optimization analysis according to constraints and objectives. The program can also be used for system identification problems or stochastic analysis. The program allows the user to monitor parallel simulations performed with LS-DYNA and a post-processing tool has been developed such that the results can be visualized [27].

ANSA.
ANSA is an advanced multidisciplinary Computer Aided Engineering (CAE) pre-processing tool that provides the functions needed to go from a CAD-file to a ready to run solver input file. ANSA is compatible with LS-DYNA and several tools for car crash analysis are implements, e.g. defining airbags or positioning of dummies. Moreover, FE geometries can simply be adjusted in ANSA by a morphing tool. The morphing tool can further be parameterized and used to quickly generate a number of alternative designs. Lastly, it is possible to couple ANSA with LS-OPT which makes it a great choice as pre-processor in this thesis [28].

META.
META is a post-processor with capabilities to do various of computations and visualize animations, figures, plots and more. It allows the user to define scripts to automate the process from simulation to report generation which is profitable when running several simulations. Moreover, it is developed by the same company as ANSA and it can also be coupled with LS-OPT [29].

3 | Method

The method is divided into several steps with four separate main sections: Define input parameters and their statistical distribution, define output parameters in terms of both risk indicators and kinematics, development and validation of generic vehicle FE model for frontal crashes and lastly a schematic description of the whole stochastic simulation process. The first section describes the essential steps in defining the relevant input parameters affecting the outcome of a frontal passenger in a frontal impact. It also describes how the information about the statistical distribution was gathered. The section is followed by the different measures of outputs available and generated to be able to understand the influence of the different input parameters. Additionally, the procedure of developing a generic vehicle model, which must be able to handle the defined input and output, and the validation of that model are described in more detail. Lastly, the process from varying input parameters, running simulations and gather outputs are summarized and explained.

3.1 Selection of input parameters

Significant variability in results can be detected when performing physical crash tests. The variability is caused by the variation of different input parameters such as dimension parameters of the safety system, material parameters of the vehicle structure as well as testing conditions. This leads to the necessity to not only evaluate the safety system with nominal values, but with the variability included as well.

3.1.1 Finding the most critical input parameters

In order to evaluate the influence of variability of the safety system, the most critical input parameters must be found and translated into an adequate statistic description. First of all, literature was used gather information about what parameters that have been used in previous studies. Secondly, several simulations ran by VCC were analyzed with the objective to see what happened to the dummy kinematics when some input variables were changed, e.g. airbag ventilation diameter or airbag trigger time. The simulations were also used to analyze which parts of the car that interacts with the passenger in a frontal impact, e.g. the floor or the seat. The critical parameters were gathered in a table, see Table 3.1. The parameters are grouped into friction values, airbag parameters which applies to both PAB and KNAB, geometry, seat, impact and occupant. Some parameters are functions of several other parameters and other parameters can be split into several parameters, for example occupant position can be split into x, y and z position.

Further, in this thesis the parameters were also defined as either a *design*, *production* or *real life* parameter. A design parameter is a parameter that VCC can vary in the design phase and the influence of the parameter show the result of different designs, e.g. a longer och shorter airbag. Further, a production parameter is a parameter that is affected by the production, e.g. manufacturing tolerances, and the distribution can be taken from measures in the manufacturing. It is often narrower compared to the design parameter. Lastly, a real life parameter is a parameter that is hard to control and depend on the specific impact situation in real life crashes, e.g. the seating position or friction between the occupant and different surfaces in the car. These parameters are difficult to both determine and control. Many parameters are a combination of two or all three types but sorting them in different types of parameters helps to understand why a certain parameter distribution was chosen.

Thirdly, a meeting with experienced engineers was held at VCC where the input parameters in the table were presented and discussed. With help of engineering judgment, the number of different input parameters was reduced to fit the time frame and scope of the project. For this project, only a few parameters were chosen to be varied to ensure that the developed method was working. Therefore, parameters considered to be outside of the project scope or where the data would take too long to gather, were set to a constant value.

Table 3.1: Input parameters affecting the outcome of a frontal impact identified in the current study.

Group	Parameter	Design	Production	Real life
Friction values	Dummy - seat			x
	Dummy - KNAB			x
	Dummy - PAB			x
	Dummy - floor			x
	Airbag self contact	x		
	Airbag - IP	x		
	Airbag - Windscreen	x		
Airbag (PAB/KNAB)	Airbag volume	x		
	Airbag width	x		
	Airbag length	x		
	Airbag impact angle towards occupant	x		x
	Airbag pressure	x	x	x*
	Airbag mass flow	x	x	
	Airbag trig time	x		x
	Fabric leakage	x	x	x*
	Fabric failure force	x	x	x*
	Initial airbag inlet temperature	x	x	x*
	Ventilation diameter	x	x	x
Geometry	Instrument panel shape	x		
	Intrusion instrument panel	x	x	x
	Intrusion Floor	x	x	x
	Floor shape	x	x	
	Windshield shape	x	x	
	Passenger door shape	x	x	
Seat	Horizontal position	x		x
	Vertical position	x		x
	Rotation around y-axis (tilted backwards/forwards)	x		x
	Seat cushion stiffness	x	x	x
Impact	Pulse	x	x	x
	Impact angle			x
	Delta velocity			x
Occupant	Occupant position in seat			x

*Airbag pressure, temperature and material properties can be real life parameters since they are affected by ambient conditions quite a lot.

3.1.2 Gather statistical distribution information

Parameters can have different parametric distributions. The simplest statistical distribution of a parameter is the uniform distribution with a minimum and maximum allowed value. For a design parameter, that can be the minimum and maximum length of a part that a certain machine can manufacture. However, the parameter may be distributed in another way, for example a tolerance can be set on a certain hole diameter which may lead to a normal or log-normal distribution. In order to draw conclusions linked to a real car project, the aim was to collect correct statistical information from suppliers and the manufacturing process. Otherwise, the parameter was assigned an assumption of a statistical distribution to still be able to see trends and correlation between parameters.

Crash Pulse

The crash pulse from a full-frontal car crash can have infinitely many different forms and is therefore a parameter that is hard to specify with a specific distribution. In this project the delta velocity, i.e. the initial velocity minus the velocity after impact, was held constant at 40 kilometer per hour. However, the crash pulse can still look very different from each other, see Figure 3.1 for a generic example where the three pulses looks different but with the same delta velocity. In order to define a variation in crash pulses, different shapes of the crash pulse were created, all with the same delta velocity but with varying Vehicle Pulse Index (VPI) [7]. VPI is the maximum dummy chest acceleration in a simple SDOF model of a sled simulation computed as

$$M\ddot{y}(t) + ky(t) = P(t) \tag{3.1}$$

$$P(t) = \begin{cases} 0, & x < s \\ k(x(t) - s), & x \geq s \end{cases} \tag{3.2}$$

$$VPI = max(\ddot{y}(t)) \tag{3.3}$$

Where M is the mass of the dummy, $\ddot{y}$ is the acceleration of the dummy, k is a spring and s is a slack representing the restraint system, $\ddot{x}(t)$ is the acceleration of the car body. Thus, the input to the model *x(t)* is the vehicle body motion. Figure 3.2 shows an illustration of the single degree of freedom model. The stiffness of the spring and the distance of the slack is parameters that VCC has defined. Using the VPI made it possible to quantify the variation and of the pulse. A reasonable range for the VPI for unbelted frontal impacts was given by engineers at VCC.

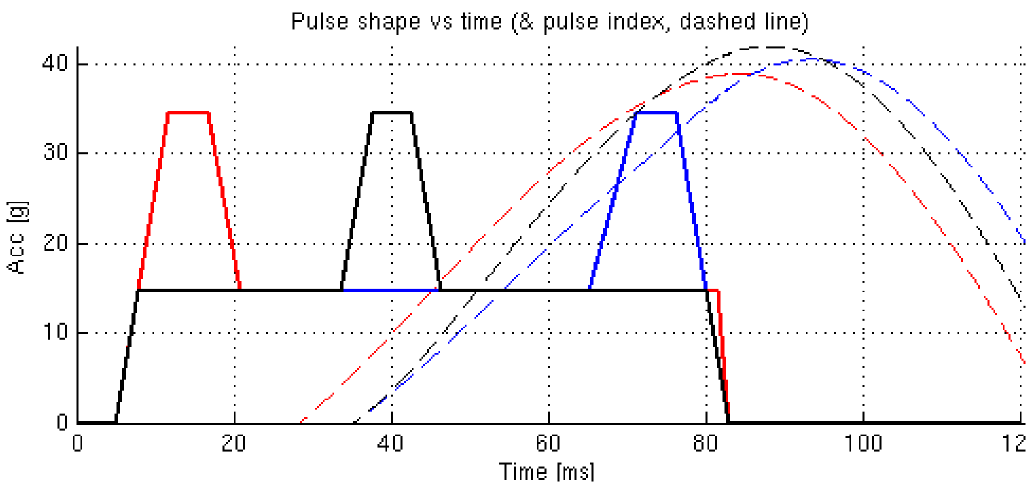

Figure 3.1: Example of three different type of crash pulses with the same delta velocity, VPI shown as dotted lines.

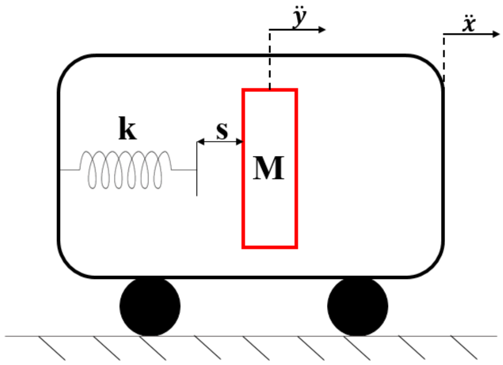

Figure 3.2: Single degree of freedom VPI model.

3.1.3 Generation of input variables

To be able to keep the amount of necessary simulations as small as possible, but still get an acceptable confidence interval, Latin Hypercube Sampling (LHS) was used. There are other methods to get good confidence with a low number of samples, but direct evaluation at the sample points using the FE model are done in this thesis, rather than using surrogate models. Hence, LHS works well. The LHS method is a constrained random sampling technique where the statistical distribution of a variable is split into N partitions with equal probability and then samples are picked randomly from each interval. The method is illustrated in Figure 3.3 where the probability density function of a single variable X is shown. The blue dots are examples of sample locations and the vertical lines are the division of the probability density function into areas of equal probability. LHS tends to produce a better estimate of the population parameter for the same number of samples compared to a total random Monte Carlo sampling. In other words, LHS requires a lower amount of samples to create similar confidence intervals as the random Monte Carlo [30, 31]. Hence, LHS was used to sample the parameter setting for the simulations.

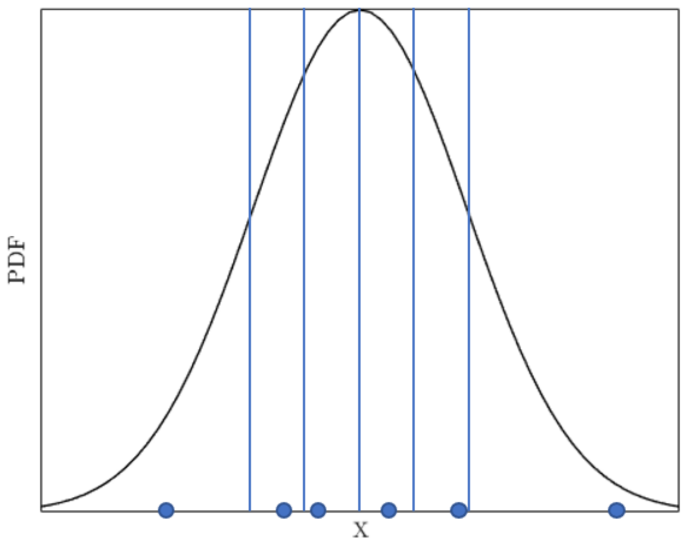

Figure 3.3: Illustrative graph of Latin Hypercube sampling for a normal distributed parameter X.

3.2 Selection of output parameters

There are many different output parameters from a crash simulation available to choose from. When the input parameters are varied, it is important that the output parameters are clear and provide the necessary information needed to draw conclusions on how the input parameter affected the occupant. Therefore, results from simulations and physical tests at VCC was studied to find these output parameters. First of all, the different risk indicators were compared between each other. Secondly, parameters regarding the kinematics of a dummy in a frontal crash were studied.

3.2.1 Dummy risk indicators

The risk indicators used as output were chosen with the similar strategy as for the input parameters, i.e. literature, simulations and test done by VCC were analyzed to find the most relevant criteria to use as outputs. A list of possible candidates was made with two restrictions in mind. First, only risk indicators which showed a clear difference when changing the input parameters of for example the airbag were used. Results from simulations with different parameter combinations given by VCC were used to decide on this. Secondly, only risk indicators available for the simplified dummy could be used for validation. Hence, only a few criteria could be used as output in the simplified model. The possible choices are listed in Table 3.2.

Table 3.2: Dummy injury risk measurments possible to use in the simulations.

Risk Indicators	**Abbreviation**
Head Injury Coef. max of 15ms	HIC_{15}
Head Injurt Coef. max of 36ms	HIC_{36}
Head acceleration 3ms	$HCLIP3m$
Chest acceleration 3ms	$CCLIP3m$
Pelvis acceleration 3ms	$PCLIP3m$
Chest deflection	Cd
Upper neck shear force	NF_x
Upper neck tensile force	NF_z
Left femur force	LFF_z
Right femur force	RFF_z

3.2.2 Dummy kinematics

To be able to understand the influence of the safety system on the occupant, it is important to not only analyze the risk indicators, but also the kinematics. If the dummy was perfect, measuring all possible injuries, the kinematics would not be important. But that is not the case and valuable information can be gathered by analyzing the kinematic. For example, if the dummy is sliding of the airbag, it may not be seen by the risk indicators, but by measuring the kinematics the unwanted behaviors can be detected. Hence, a method to measure the most important movements of the dummy was developed. Data from simulations and videos from physical testing done with the wanted load case were gathered to get an understanding of how the dummy is moving during a crash sequence. As an example, an FE simulation of the primary load case is used. The general kinematics in a crash sequence can be seen in figure 3.4 where the dummy is shown from the side. The crash sequence can be divided into different steps:

1. The car and everything inside it are moving with the initial velocity.
2. The car starts to decelerate due to impact and the airbags are deployed.
3. Since the dummy is not wearing any belt, the dummy is free flying forward.
4. The feet are stopped by the floor which makes the tibia bone rotate forward.
5. Knees impact in the knee airbag, making the chest and head rotate forward.
6. Chest and head are captured by passenger airbag and the motion is slowed down.
7. The dummy is either stopped completely or the dummy bounces back in the opposite direction.

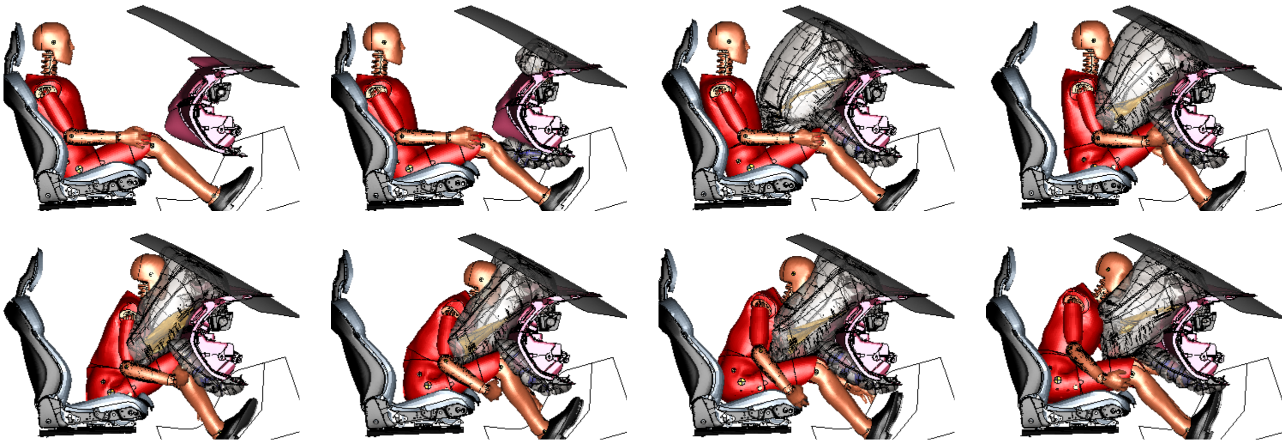

Figure 3.4: The kinematic for an unbelted dummy in a frontal impact simulation. Time stamps (ms): 0, 20, 40, 60, 80, 100, 120, 140.

It is clear that different parts of the dummy interact with the surrounding at different time. Thus, one movement leads to another. For example, the knee impact in the instrument panel or knee airbag results in the chest rotates forward. In this specific load case, the main movement for the dummy is displacement in X direction and rotations around the Y and Z axis (angles measured in the ZX and XY plane).

A human body or dummy is limited in rotation by different joints. Hence, it is possible to visualize how the dummy is moving by measuring the rotational angle in the joints connecting the larger body parts, e.g. knee-joint and hip-joint. Also, rotation of the head is important. The arms are connected to the shoulder-joint, but they are assumed to have little influence if placed in standard position, i.e. along the side of the body.

The method to measure kinematics was developed in the FE model presented above. Since it is a computer simulation, endless opportunities to measure displacement and angles exists. A META script was developed to compute different angles between chosen nodes in the model, see Table 3.3. The measured kinematics were divided into; rotations around the Y-axis, rotations around the Z-axis and displacement of center points which is explained in more detail below.

Table 3.3: Numbering of measured rotation angles around the global Y and Z axis.

Rotation around global axis	Angle	ID
Y	Left and right Tibia vs Floor	1
	Left and right Tibia vs Femur	2
	Left and right Femur vs Chest	3
	Chest vs Head	4
Z	Centre of Pelvis	5
	Centre of Chest	6
	Centre of Head	7

3.2.3 Rotation around the Y-axis

The rotation around the Y-axis in frontal crash depends on the interaction with the seat, floor, instrument panel or KNAB and PAB. It is mostly common that the rotation starts from the lower part of the body and is therefrom passed on trough the pelvis, chest and finally the head. Hence, it is of interest to see how the different body parts are rotating during the sequence of a frontal crash. The four different angles that are outputted from the developed script are illustrated in Figure 3.5 where a cut trough a stripped dummy is shown in a sitting position. The angles are measured for both the left and right leg.

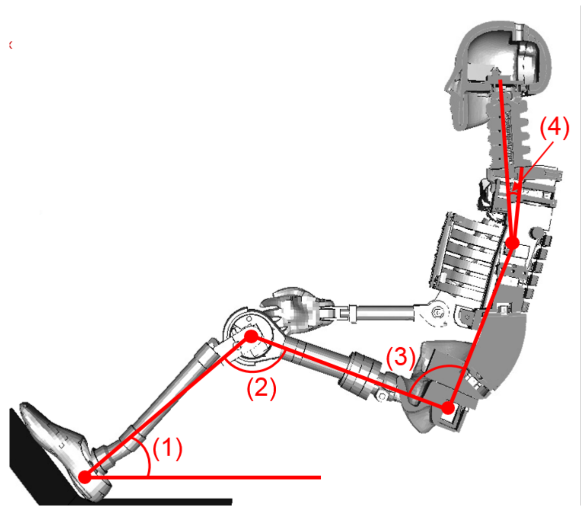

Figure 3.5: Illustration of measured rotational angels around the global Y-axis.

3.2.4 Rotation around the Z-axis

A full-frontal impact does not contribute to any significant initial rotations around the global Z-axis of the occupant, thus the rotation depends on the interaction with the surroundings. As an example, if one of the knees meets the KNAB before the other, a rotational movement will start and move through the different parts of the body. The rotation around the Z-axis is evaluated in three different points, i.e. center of pelvis, center of chest and center of head. This is visualized in various plane cuts on a dummy in Figure 3.6.

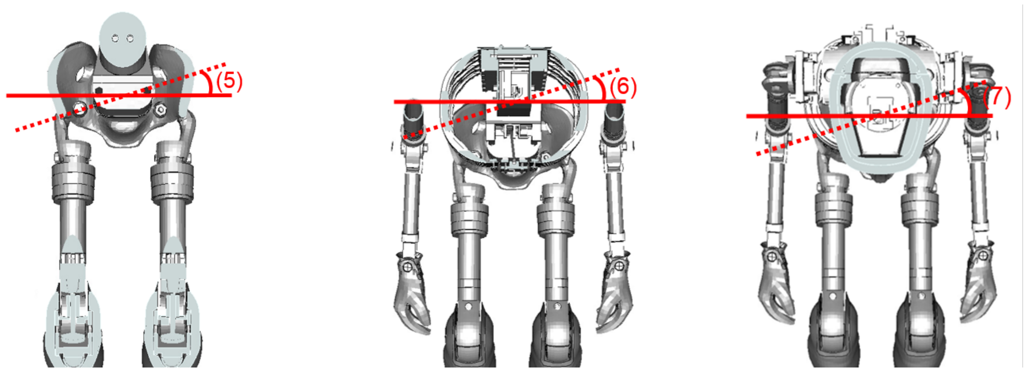

Figure 3.6: Rotation around Z for various plane cuts, i.e. center or pelvis (left), center of chest (middle) and center of head (right).

3.2.5 Displacement of centre points

Even if the rotational angles are the same for two different simulations, the kinematics of the dummy can still vary, i.e. the total displacement can be different. Therefore, the displacement of center dummy head, chest and pelvis is monitored in X, Y and Z direction.

3.2.6 Responses and histories

The different outputs were also divided into responses and histories. Histories are curves based on time data obtained from the simulations. However, it is not possible to compute statistical distributions or correlation analysis from a curve with time depending values. For example, the correlation between two variables must be computed with distinct values. Hence, responses are defined as only one value per simulation and can be used for this type of computations. As an example, the head displacement in X direction can be plotted over time and is defined as a history, while the maximum head displacement in X during the simulation is only one value, and therefore defined as a response.

3.3 Development and validation of generic vehicle FE model for frontal impact

In order to understand how a variation of input parameters mentioned in previous sections regulates the output, many simulations need to be performed. Hence, a simplified generic FE model for frontal impact was needed. The model was intended to maintain the predictive capability of the detailed FE model whilst retaining a parametric representation of the input parameters decided to vary. The model had to be simple in the terms of computation cost but still validated against the more detailed model. The model is based on a reference FE model at VCC and it is also that model which the simplified model is validated against. A flowchart over the process is shown in Figure 3.7.

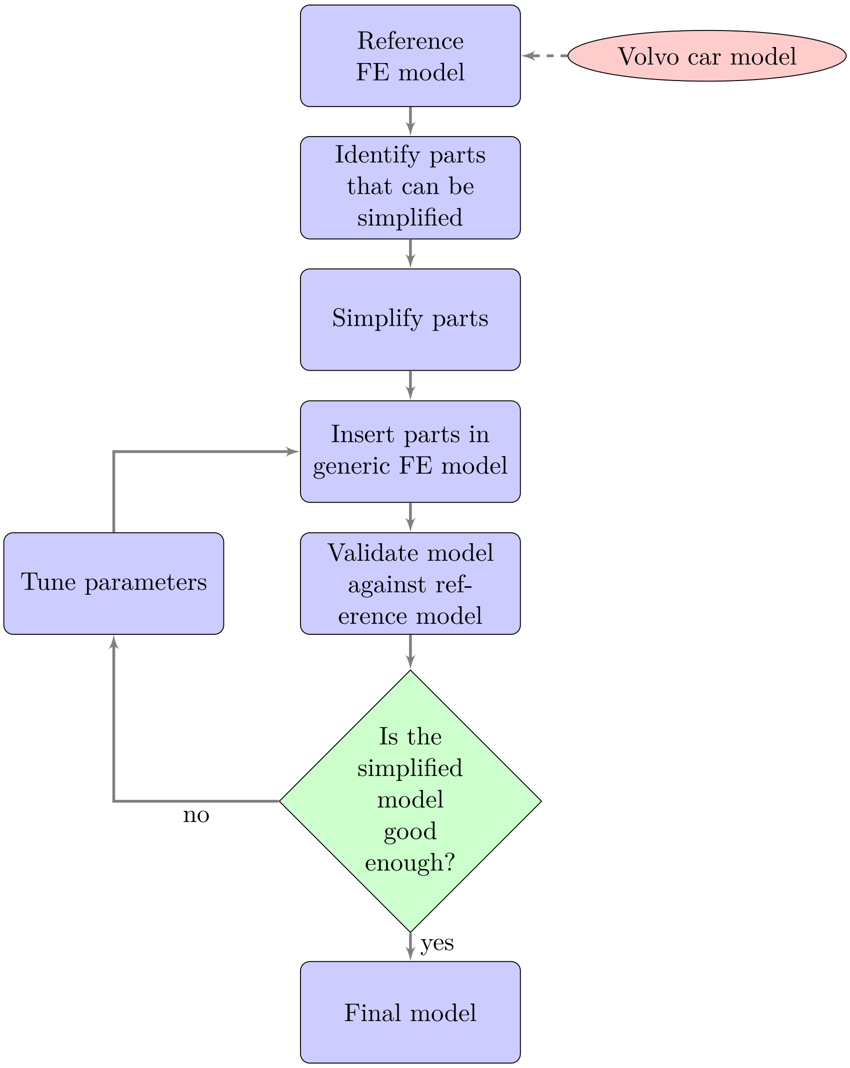

Figure 3.7: Flowchart over the development and validation of generic vehicle FE model.

3.3.1 Description of Reference model

The model referred as the *reference model* in the thesis report is an FE model received from VCC. It has been used in internal studies and is shown in Figure 3.8. The model is a combinations of parts from different car projects with some modifications and simplifications. Due to that it exist confidential information in the model used at VCC, a different instrument panel already in production is shown in the report. Thus, the housing of the PAB looks a little miss-placed. Furthermore, the model is design for the frontal passenger and full-frontal impact, this version has no belt included, but both PAB and KNAB which is the same setup that the simplified model in the thesis is aiming for. Hence, the simulations already ran by VCC with the reference model was used for the validation of the simplified model.

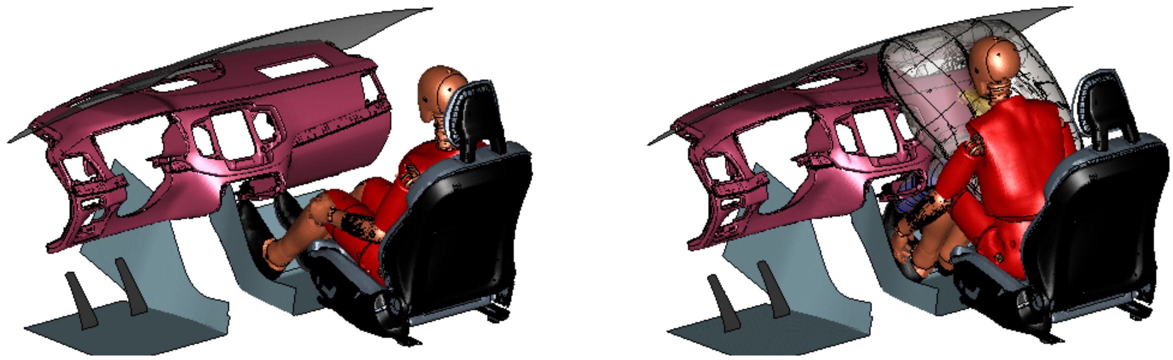

Figure 3.8: Reference model in frontal impact simulation, time step 0 ms (left) 80 ms (right).

3.3.2 Create a simplified, parameterized vehicle FE model

The most important parts to include in the model for this project of the vehicle interior are the parts that the frontal passenger get in contact with during a crash sequence. Both the geometry and stiffness of the impact surfaces as well as properties of the airbag system are of great importance. The main parts to include was PAB, KNAB, windscreen, floor, instrument panel and seat. The geometry of the generic model were either build from scratch with the detailed model as reference or surfaces were extracted from the reference model.

Passenger airbag.
The passenger airbag was modelled with two sides connected with a strap. The two sides control the main shape of the airbag and the strap decides the width. Moreover, the simplified airbag was design to look like the reference PAB fully inflated. The main simplification is that the airbag is not folded, it is inflated in the unfolded stage from the start. Further, the shape is edgy so that the sides can be parameterized. The backside of the airbag is defined as a rigid surface to represent a part of the instrument panel. The other parts were modeled as a coated woven fabric material. A coated material was chosen to give better control of the leakage since leakage occurs through the ventilation hole only. The nominal PAB with a volume of 100 liter is shown both uninflated and inflated in Figure 3.9. Included into the model was also a ventilation hole where the area of the whole is parameterized. Lastly, the airbag is modeled with the LS-DYNA AIRBAG_HYBRID keyword.

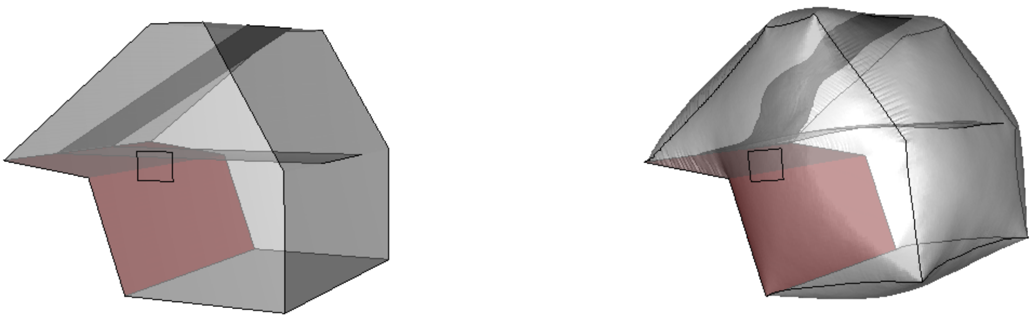

Figure 3.9: Simplified uninflated PAB (left) and inflated (right).

The gas generator and mass flow was first modelled as a discontinues curve with the trigger time $t = t_0$, maximum peak $\dot{m}_{max}$ at $t = t_1$ and end of mass flow at $t = t_2$. As a starting point, the three variables and peak mass flow was chosen such that the amount of gas (mass) was the same as for the reference PAB, i.e. the integral of the mass flow curve where the same. Figure 3.10 shows the mass flow of the reference model together with the parameterized.

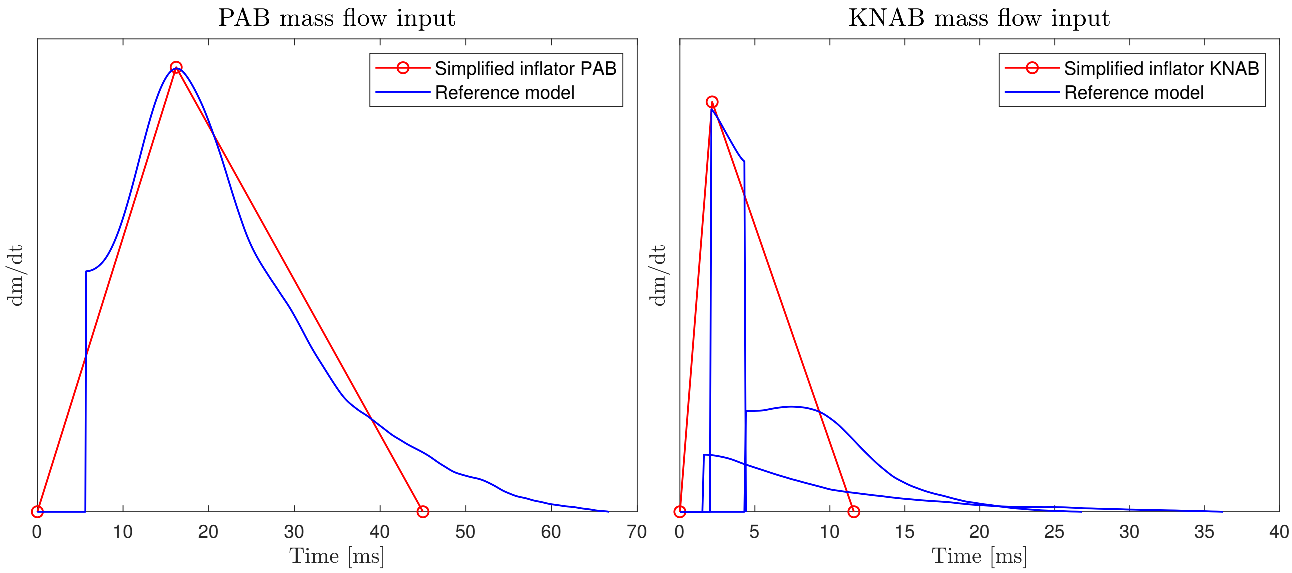

Figure 3.10: Simplified parameterized inflator for PAB (left) and KNAB (right).

Knee airbag.
The knee airbag was developed very similar to the PAB, but the shape is even more simplified. It has a rectangular shape and two straps inside such that the bag keeps its rectangular shape. The backside is defined as rigid and is angled to represent the lower part of the instrument panel. The other parts were modeled as a woven uncoated fabric material where leakage through the fabric occurs depending on the pressure inside the bag. The nominal KNAB with a volume of 20 l is shown both uninflated and inflated in Figure 3.11. At last, the airbag inflator and mass flow was defined in the same way as for the PAB but with the detailed KNAB as reference, see Figure 3.10. The reference inflator for the KNAB is modeled with three different gases inflating the airbag at different starting times. However, the simplified model uses only one gas.

Figure 3.11: Simplified uninflated KNAB (left) and inflated (right).

Windscreen and floor.
The windscreen and floor are surfaces extracted from a Volvo car model. Only the part that the feet may interact with in a frontal impact was simplified and the rest was removed. Further, the windscreen was split in half such that only the part in front of the passenger was used. Lastly, both the surfaces were assumed rigid.

Seat.
An FE model of a seat can be extremely complex consisting of many parts with detailed material models, e.g. different foams and plastics, joints and internal contacts. Moreover, bolt connections are often pretensioned, which is set up during the initial stage of the simulation. Hence, the seats used at VCC for FE simulations are computer costly. The seat was modified to fit the purpose of this project with changes such as new contacts, connections and several parts where removed, e.g. the foam of the backrest, plastic parts, electric engines controlling the seating position, see Figure 3.12. The changes were made using the reference model and study each part to see if it affected the behavior of the seat. As an example, if two parts connected with a pretensioned bolt did not rotate during the impact, the connection was modeled with a rigid constraint instead. Another example is parts made only for visual effects which were removed if they did not contribute to the structural stiffness.

Dummy.
A simplified Hybrid III crash test dummy model called FAST50, developed by LSTC was used, see Figure 3.13. The dummy is modeled with large finite elements and has less post-processing opportunities compared to the detailed LSTC HIII dummy. Moreover, the dummy was seated in the seat during a pre-processing stage in ANSA. The dummy is simulated down in the seat which results in the seat foam is being deformed. This deformation was saved and used as initial deformation gradient in simulations.

Figure 3.12: Simplified seat model.

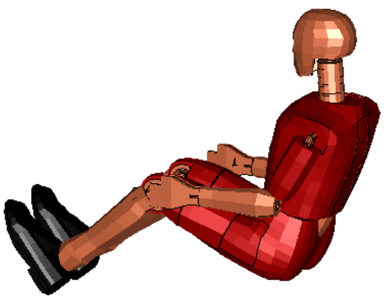

Figure 3.13: LSTC FAST50 version 2.0 dummy.

All simplified models together.
The complete simplified FE model is shown in Figure 3.14. Potential contacts between the dummy and seat, airbags and floor were defined, also contact between the airbags and the PAB versus the windscreen was included in the model. The contacts were modeled as contacts with CONTACT_AUTOMATIC_SURFACE_TO_SURFACE. All rigid parts are constrained to a single node where the prescribed motion of the pulse is applied.

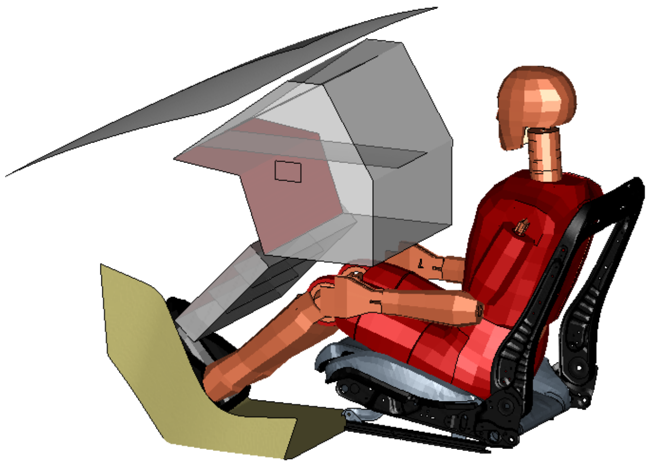

Figure 3.14: Developed simplified frontal passenger FE model.

3.3.3 Validation of the simplified model

Validation of the simplified model was done by comparing each component to the same sort of component in the reference model in a one to one test. Each detailed component in the reference model where exchanged with the corresponding simplified component and then a frontal impact simulation was run. The exact same pulse for both the complete reference model and reference model with one of the simplified components was used such that the results could be compared.

The tests were ran for the PAB, KNAB, seat and dummy but only the two first components were used for tuning. For all simplifications, risk indicators were extracted to see differences between the simplified and detailed models. Also, the kinematic behavior of each component were studied through the simulations. In this project, the procedure was done two times, first one time before the parameters where tuned by curve fitting in LS-OPT and then one time afterwards to see if the quality of the model had improved. Given more time, this step can be repeated several times and more parameters could be tuned.

3.3.4 Tune parameters by curve fitting in LS-OPT

Tuning parameters can be very time consuming, especially in a crash analysis since the analysis is non-linear and effects of the parameter changes can be tough to predict. Moreover, design objectives, e.g. lowest possible mass or maximum strength is often in conflict with each other. Therefore, mathematical objective functions depending on design choices made can be developed and subjected to optimization. In this case, a curve fitting approach was used.

LS-OPT is an optimization software with built in functionality to handle both single and multiple objective optimization. The tool can also be coupled with several pre-processors, solvers and post-processors. In this section, the method to set up the PAB, KNAB and seat parameter tuning as an optimization task will be described.

First, a decision on which objective functions to use was made together with which parameters should be manipulated to influence the functions. Secondly, the FE model must be parameterized either by using the pre-processor ANSA and an optimization task or by defining parameters in the LS-DYNA FE input files. Further, the LS-DYNA output requested by the optimization must be defined. Lastly, LS-DYNA is running at a computing cluster at VCC, LS-OPT can therefore not run LS-DYNA directly. Instead, a Phyton script that submits the LS-DYNA job into the cluster queue is called upon in LS-OPT and used to run the tasks.

Optimization task for simplified PAB and KNAB.
The FE models of the PAB and KNAB can both be tuned to get a behavior more like the detailed airbags in the reference model. The contact force between the airbag and the dummy must be in a reasonable range in order to draw trustworthy conclusions from the simplified model. Therefore, an optimization task in LS-OPT was used. The optimization task is based on the frontal impact simulations performed with the reference model,

Objective function.
In order to perform an optimization task, data representing the true system is needed. The pressure of the airbag has a large impact on the interaction between the dummy and airbag. It will determine how stiff the airbag is and how high the force between the knees and KNAB and the head and chest against the PAB will be. If the pressure in the simplified models can be set-up to obtain the same calculated pressure when the dummy is impacting the airbags in a frontal impact, this would mean that the simplified airbag has similar behavior as the reference model. Of course, other factors influence the system as well, e.g. size and shape, but they are assumed to be accurate enough since the bag has the same volume and the overall contact with the dummy was as close as possible for an unfolded airbag. As the objective function, a curve fitting function that measured the root mean square error between the time histories of the reference airbag pressure and the simplified airbags was used. Hence, if the error is zero, the two curves would be identical. Thus, the objective function shall be minimized by changing the defined parameters in the simplified model.

Parameter set-up.
There are many different parameters to use to tune the pressure of an airbag, e.g. temperature, size, ambient pressure, mass flow, etc. In this project, the mass flow of the simplified inflator where used as tuning parameters. The tunable parameters where mass flow peak $\dot{m}_{max}$ and the two time settings t_1 and t_2. Constraints on the parameters where set to the parameters to prevent that they did not end up beyond reasonable limits. The mass flow limits for PAB and KNAB were set to $0.5 < \dot{m}_{max} < 3.5$ and $0.5 < \dot{m}_{max} < 6.0$ respectively. The timing for the different points on the curve were set as $t_2 > t_1 + 10$ ms and $t_1^{initial} < t_1 < 45$ ms for the PAB and $t_1^{initial} < t_1 < 35$ ms for the KNAB.

Optimization.
The optimization task used in LS-OPT for this is a metamodel based optimization. A metamodel-based optimization is used to create and optimize an approximate model of the FE model instead of optimizing the design through direct simulation. One can say that the metamodel is created as a inexpensive surrogate of the actual FE model and is therefore less expensive to optimize compared to the actual FE model. Hence, less simulations needs to be run. The recommended settings in LS-OPT

was used with a linear polynomial metamodel. A flowchart of the optimization procedure can be seen in Figure 3.15.

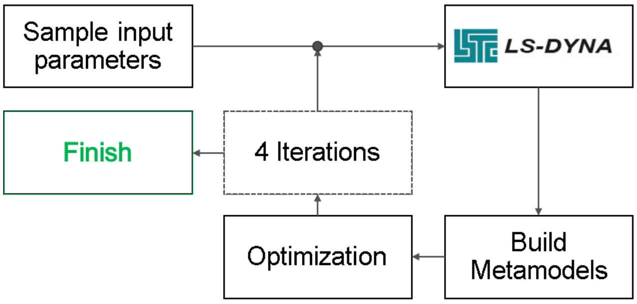

Figure 3.15: A flowchart of optimizing pressure curve for simplified PAB in LS-OPT.

The final step after tuning the airbag parameters was to once again validate the simplified model against the reference model to see differences. In order to draw reliable conclusions about trends between input and output parameters, the model must show similar behavior as the reference models which have been evaluated against physical testing. More loops of validation and tuning can be done but was said to be outside of this project due to the time limit. Hence, the final simplified model was assembled and ready for the stochastic simulations.

3.4 Stochastic simulation set up

The first step in this phase was to set up the simplified model with the chosen input parameters. Further, test the robustness of the simplified model by running a few designs in the extreme corners of the chosen design space. In other words, the designs were run with the design variables set to their minimum and maximum values. The results were analyzed and the input parameters where modified if needed for the full analysis.

Secondly, a Monte Carlo analysis was used to simulate the uncertainty of the variables using random samples based on the associated distributions of the defined input parameters. In this analysis, a metamodel based analysis was included as well, meaning that the Monte Carlo analysis was also done using metamodels. Latin Hypercube Sampling was used to sample the parameter settings for each of the 150 simulations. For every simulation, the Monte Carlo evaluation does the following:

- Select the random sample points according to LHS and the statistical distribution assigned to the input parameters.
- Evaluate the simulation of the frontal impact.
- Collect the statistics of the defined output.

The metamodel is constructed based on the results from the samples evaluated from the simulations. Further, 10 million samples are generated and computed with the radial basis function based metamodel, making it possible to evaluate more statistics. However, the results from the metamodel must be handled with caution since it is an approximation of the real model. The Monte Carlo simulation was set up in LS-OPT and can be visualized in a flowchart in Figure 3.16.

Statistical data such as mean, standard deviation, correlation and sensitivity were computed for all inputs and outputs. The data was first visualized in a correlation plot between all selected parameters to get an overview of which parameters influence each other and which does not. Secondly, scatter plot of some of the interesting results was made. Lastly, the history curves were plotted based on time data or cross plots obtained from simulations. Together, all these different ways of showing the results can help to get an understanding of the defined system.

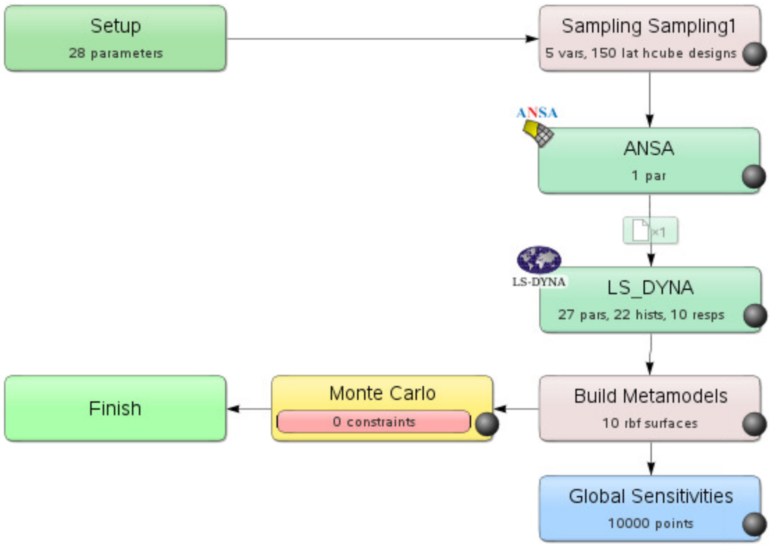

Figure 3.16: An LS-OPT flowchart of the metamodel-based Monte Carlo analysis for the simplified FE model.

4 | Results

In this chapter, the selected input parameters and their corresponding statistical distribution are presented. Furthermore, the selected outputs are listed and commented. The model validation and parameter tuning are performed and the differences between the simplified model and reference model are shown. Lastly, the stochastic simulations are executed and the resulting statistics from the simulations are summarized. Not all plots were shown, and the figures presented were chosen either because they were assumed to be a good example of how the method can be used or if they showed an interesting result.

4.1 Selected input parameters

In total, five parameters have been chosen to be varied in the simulations. The first set of parameters were chosen mainly to examine how well the method is working. Furthermore, at least one parameter from each type is included in the parameter set. Also, parameters that are uniform and normal distributed and discrete are included. The selected input parameters to vary in the study are presented with each statistical distribution in Table 4.1.

Table 4.1: Summary of selected input parameters and distributions used in the stochastic simulation.

Parameter	Type	Unit	Distribution	Distribution parameters
PAB length in X-dir.	Design	[mm]	Uniform	min=540 , max=640
PAB inflator mass flow peak, $\dot{m}_{max}$	Design	[kg/s]	Uniform	min=0.85, max=1.27
PAB ventilation diameter	Production	[mm]	Normal	$\mu = 50$, $\sigma = 1.0$
Crash pulse (VPI)	Real life	[g]	Discrete*	min=37.3, max=45.8
PAB - Dummy friction	Real life	[-]	Uniform	min=0.1, max=0.6

The two design variables are the PAB length in X-direction and the inflator mass flow peak. The PAB length in X-direction controls the length of PAB in the uninflated state. Hence, it is a parameter that makes it possible to see the influence of the airbag coming closer to the occupant which results in an earlier contact in the crash sequence. The inflator mass flow peak is set to the tuned value $\pm 20\%$. The only production related variable is the PAB ventilation diameter which is set to the nominal value of 50 mm and a standard deviation of $\sigma = 1$ mm which is values used at VCC.

The VPI of the crash pulse is extracted from 28 pulses with different shapes. The pulses are defined by different curves with varying VPI, and the curves are chosen with discrete steps. Hence, the crash pulse min and max value only refers to the VPI and does not say anything about the shape. The exact data sheet for the pulses including: VPI, delta velocity, stopping distance and pulse end time can be found in Appendix A. In addition, there are more curves with a VPI close to the mean value. Further, the 28 pulses defined are the only available, meaning that the exact same pulse is simulated several times.

Lastly, the friction coefficient between the PAB and the dummy is unknown and therefore set to a uniform distributed parameter between 0.1 and 0.6. Other parameters were set to constant values given from the reference model, e.g. seat position, or parameter tuning, e.g. KNAB parameters.

4.2 Selected output parameters

The output parameters chosen to extract from the stochastic simulation are presented in Table 4.2. It is a combination of responses and histories and consists of risk indicators, kinematics and airbag data.

Table 4.2: Summary of all outputs from the stochastic simulation, sorted in responses and histories.

	Measure	Max/Min	Units
Responses	HIC15	Max	[-]
	HCLIP3m	Max	[g]
	HIC36	Max	[-]
	Chest deflection, Cd	Max	[mm]
	CCLIP3m	Max	[g]
	PCLIP3m	Max	[g]
	Upper neck shear force, Fx	Max	[kN]
	Upper neck tensile force, Fz	Max	[kN]
	Head displacement in X	Min	[mm]
	Head rotation around Z	Max(abs)	[deg]
	Chest rotation around Z	Max(abs)	[deg]
	Pelvis rotation around Z	Max(abs)	[deg]
	Angle Left Tibia - Floor	Max	[deg]
	Angle Right Tibia - Floor	Max	[deg]
	Angle Left Tibia - Femur	Min	[deg]
	Angle Right Tibia - Femur	Min	[deg]
	Angle Left Femur - Chest	Min	[deg]
	Angle Right Femur - Chest	Min	[deg]
	Angle Head - Chest	Min	[deg]
Histories	Head acceleration	-	[g]
	Chest acceleration	-	[g]
	Pelvis acceleration	-	[g]
	Head displacement in X	-	[mm]
	Head displacement in Y	-	[mm]
	Head displacement in Z	-	[mm]
	Chest displacement in X	-	[mm]
	Chest displacement in Y	-	[mm]
	Chest displacement in Z	-	[mm]
	Pelvis displacement in X	-	[mm]
	Pelvis displacement in Y	-	[mm]
	Pelvis displacement in Z	-	[mm]
	Head rotation around Z	-	[deg]
	Chest rotation around Z	-	[deg]
	Pelvis rotation around Z	-	[deg]
	Angle Left Tibia - Floor	-	[deg]
	Angle Right Tibia - Floor	-	[deg]
	Angle Left Tibia - Femur	-	[deg]
	Angle Right Tibia - Femur	-	[deg]
	Angle Left Femur - Chest	-	[deg]
	Angle Right Femur - Chest	-	[deg]
	Angle Head - Chest	-	[deg]
	Chest deflection, Cd	-	[mm]
	Left Femur force, Fz	-	[kN]
	Right Femur force, Fz	-	[kN]
	Airbag pressure	-	[MPa]

4.2.1 Kinematics

As mentioned in the method, both displacements and rotational angles of the dummy are extracted as output. Further, all the angles are computed as change in angle, i.e. the initial angle is the reference angle and the angles are computed relative to that one. Thus, all angles start at zero degrees. An illustration of the computed angles is shown for a nominal run of the load case in Figure 4.1. The rotations around the Z axis will always be small in this load case due to the pulse is applied in X direction only. Sometimes the different body parts will be rotated to the left, i.e. positive angle and sometime to the right. Hence, the maximum of the absolute value is measured as the response. Further, the angle between the tibia and floor will always increase while the angle between tibia and femur, femur and chest, and head and chest will decrease for this load case. Note that a negative value of the head versus chest angle describes the motion that the neck is bent backwards.

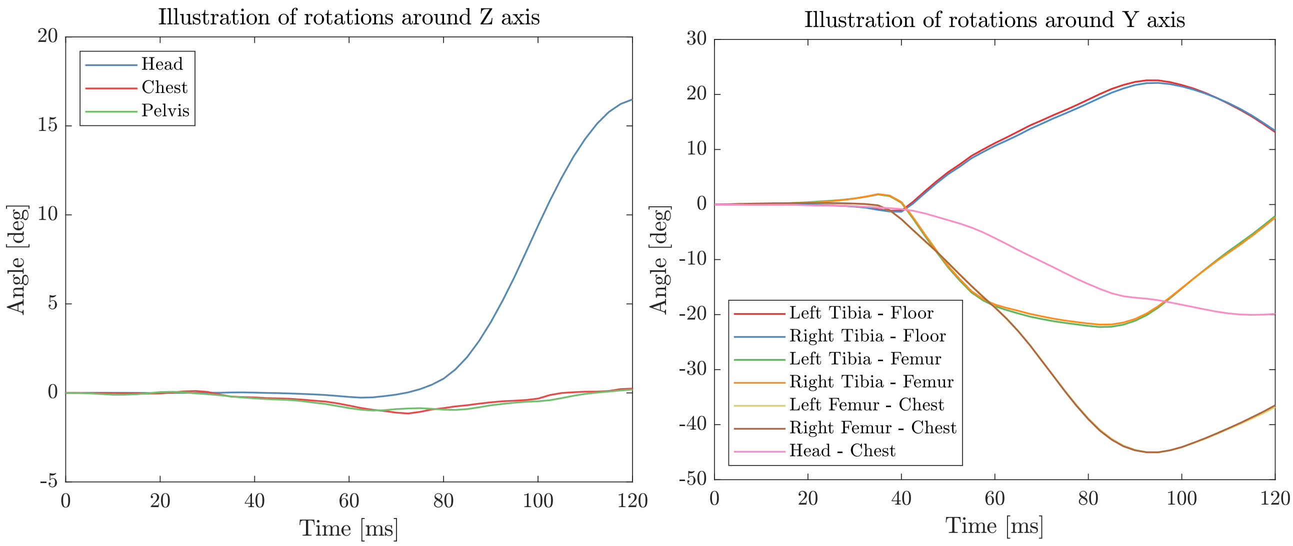

Figure 4.1: History plot of head, chest and pelvis rotations around Z axis (left) and angles between left and right tibia - floor, tibia - femur, femur - chest and head - chest (right).

4.3 Model validation

First, the results from the one to one test of the dummy are presented followed by the PAB, KNAB and seat results before tuning. After that, the results of the parameter tuning are shown. Lastly, the results from the tuned models are compared in a new one to one test.

4.3.1 One to one comparison before tuning parameters

Reference model with FAST50 dummy.
Interestingly, there were no large differences in the kinematics of the simplified LSTC FAST50 dummy versus the more detailed LSTC Hybrid III 50th percentile male dummy. The kinematic of the dummy is shown from a side and top view in Figure 4.2. On average, the dummies are moving similar to each other. However, the simplified dummy appears to be stiffer than the detailed dummy. For instance, the rotation of the chest and head is less.

Turning now to the risk indicators, the differences in HIC15, Chest acceleration and Chest deflection are presented in Table 4.3. The error lies between 4 and 17 percent depending on the criteria. However, the simplified dummy is limited in the amount sensors used for computing risk indicators which of course is a drawback.

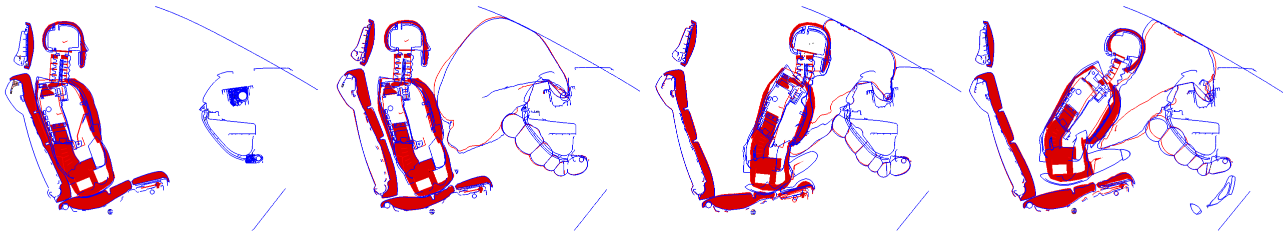

Figure 4.2: Dummy kinematic comparison between detailed dummy (blue) and simplified dummy (red). Time steps: 0 ms, 40 ms, 80 ms and 120 ms.

Table 4.3: Risk indicator comparison between LSTC FAST50 dummy (simple) and Hybrid III 50th (reference).

Model	HIC_{15} [-]	**Error**	$CCLIP3m$ [g]	**Error**	Cd [mm]	**Error**
Reference	425	-	51.1	-	18.6	-
FAST50	371	13%	49.2	4%	15.5	17%

Reference model with simplified PAB.
Moving on to the simplified PAB, the difference in kinematic is presented with a sliced cut in the ZX-plane and the view from the side in Figure 4.3. By comparing the last two time steps, it can be seen that the simplified PAB is way harder compared to the reference and the dummy is bouncing back into the seat. It can also be seen from data in Table 4.4 where the head acceleration and chest deflection are way too high due to the airbag being too stiff.

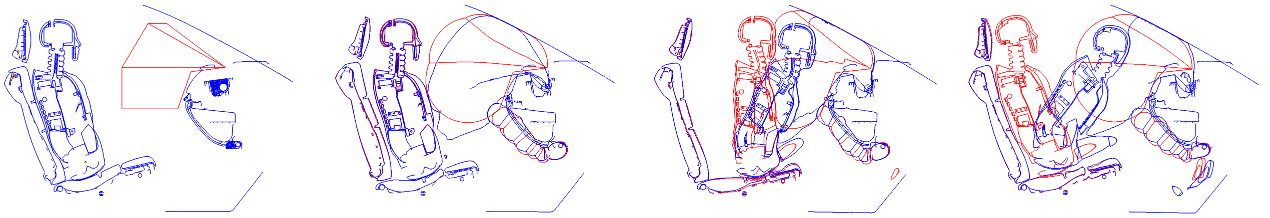

Figure 4.3: Dummy kinematic comparison between reference PAB (blue) and simplified PAB (red). Side view with slice cut in the middle of the dummy. Time steps: 0 ms, 40 ms, 80 ms and 120 ms.

Table 4.4: Risk indicator comparison between reference and simplified PAB before tuning.

Model	HIC_{15} [-]	**Error**	$CCLIP3m$ [g]	**Error**	Cd [mm]	**Error**
Reference	425	-	51.1	-	18.6	-
Simplified PAB	848	100%	61.5	20%	38.9	109%

Reference model with simplified KNAB.
The kinematic difference for the simplified KNAB compared to the reference model is presented in a similar fashion as the PAB in Figure 4.4. However, the cut in ZX-plane is through the knee of the dummy to better visualize the knee impact in the KNAB. From the last two time steps, it can be seen that the dummy in the reference model is moving more forward compared to the simplified model. The comparison in risk indicators are also provided in Table 4.5.

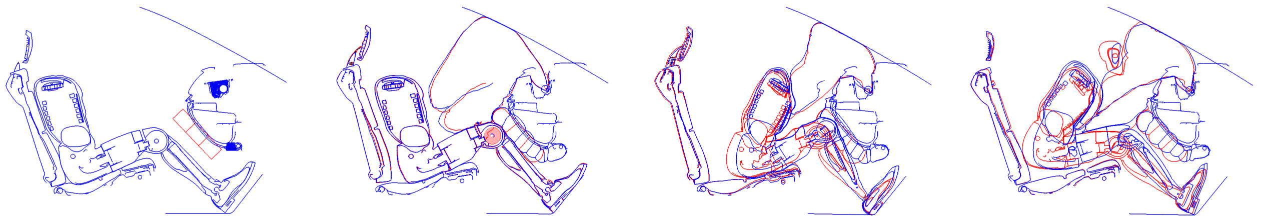

Figure 4.4: Dummy kinematic comparison between reference KNAB (blue) and simplified KNAB (red). Side view with slice cut in the middle of the dummy knee. Time steps: 0 ms, 40 ms, 80 ms and 120 ms.

Table 4.5: Risk indicator comparison between reference and simplified KNAB before tuning.

Model	HIC_{15} [-]	**Error**	$CCLIP3m$ [g]	**Error**	Cd [mm]	**Error**
Reference	425	-	51.1	-	18.6	-
Simplified KNAB	491	16%	56.3	10%	20.5	10%

Reference model with simplified seat.
Lastly, the results from the one to one comparison of the seat are presented in Figure 4.5 and Table 4.6. The figure compares the kinematics of the dummy for the simplified seat and the reference model. The view is the same as for the KNAB, i.e. a cut in ZX-plane through the middle of the knee of the dummy.

It can be seen clearly from the figure that the dummy placed in the simplified seat moves very similar to the reference, i.e. They blue and red lines are overlapping each other. Moreover, Figure 4.6 shows the seat and dummy contact forces in X, Y and Z-direction for the reference and simplified model and Table 4.6 presents the risk indicators. The difference between the two different models is relatively small. Hence, there was no need for tuning this model any further.

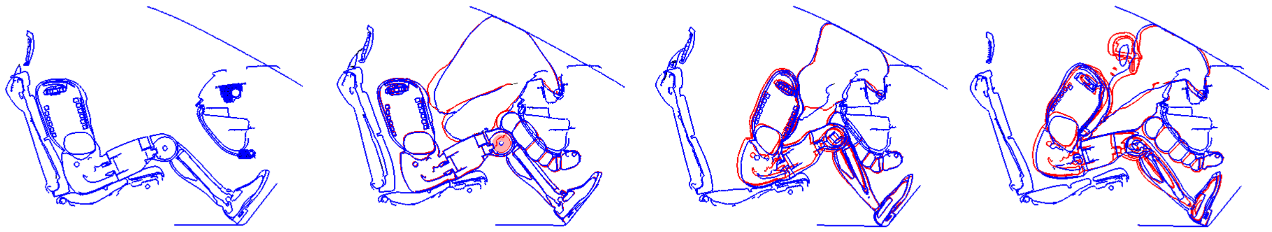

Figure 4.5: Dummy kinematic comparison between reference seat (blue) and simplified seat (red). Side view with slice cut in the middle of the dummy knee. Time steps: 0 ms, 40 ms, 80 ms and 120 ms.

Table 4.6: Risk indicator comparison between reference and simplified seat.

Model	HIC_{15} [-]	**Error**	$CCLIP3m$ [g]	**Error**	Cd [mm]	**Error**
Reference	425	-	51.1	-	18.6	-
Simplified seat	380	11%	49.5	3%	16.4	12%

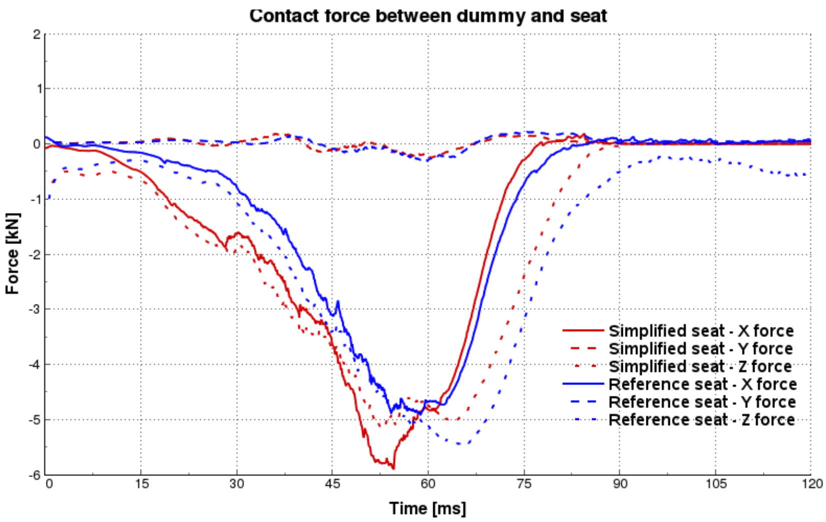

Figure 4.6: Comparison of seat and dummy contact forces between reference model and simplified model.

In brief, the main results from the first iteration of one to one testing of the simplified components are the following:

- **Dummy.** The dummy is a little bit to stiff compared to the reference. However, no tuning of the dummy is done.
- **PAB and KNAB.** Both airbags turned up to have to high pressure inside which made the contact force with the dummy to high.
- **Seat.** The seat correlated well to the reference model. Hence, no tuning of the seat is done.

4.3.2 Parameter tuning in LS-OPT

As mentioned in the method, the results from the one to one testing of the different parts are the basis for the parameter tuning. The PAB and KNAB are optimized to be more like the reference model.

The pressure in the PAB for each of the simulations performed in the optimization is presented to the left in Figure 4.7. The colors indicate different values on the maximum inflator mass flow and the target pressure is shown in black. The right figure is the pressure calculated by the metamodel. Once again, the color shows the resulting pressure with different values on the inflator. In contrast, the metamodel shows more possible outcomes since it is the result from more simulations.

The same type of results are shown for the KNAB in Figure 4.8 with the target pressure in black. From both the PAB and KNAB, it can be seen that the target pressure cannot be reached exactly. In other words, with the shape and parameter settings of the simplified airbags, a difference between the simplified model and the reference model in terms of pressure in the airbag will always exist.

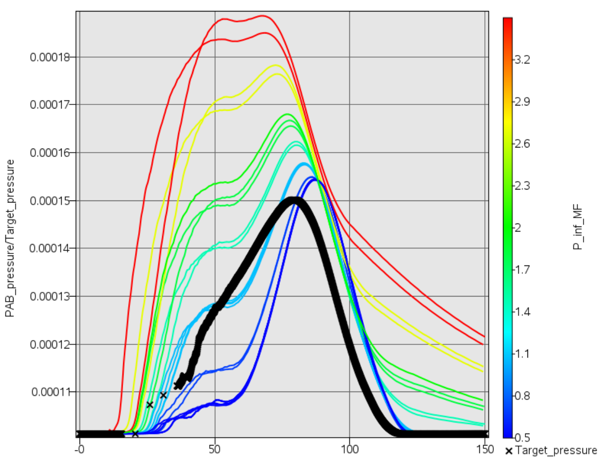

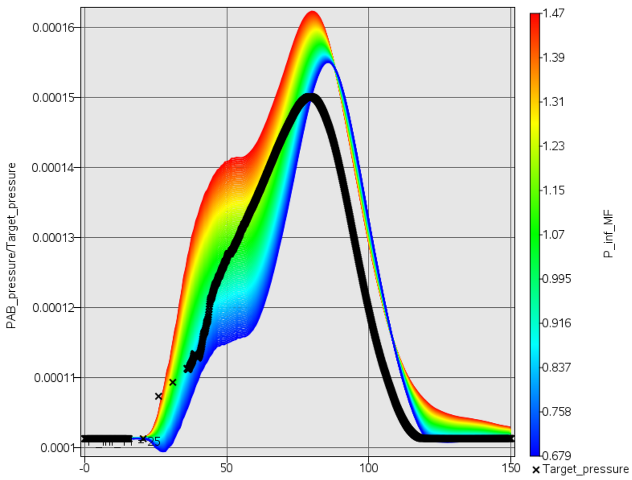

Figure 4.7: PAB pressure optimization with colors showing different values on inflator mass flow peak $\dot{m}_{max}$ and target curve presented in black. Simulations without metamodel (left) and results from metamodel (right).

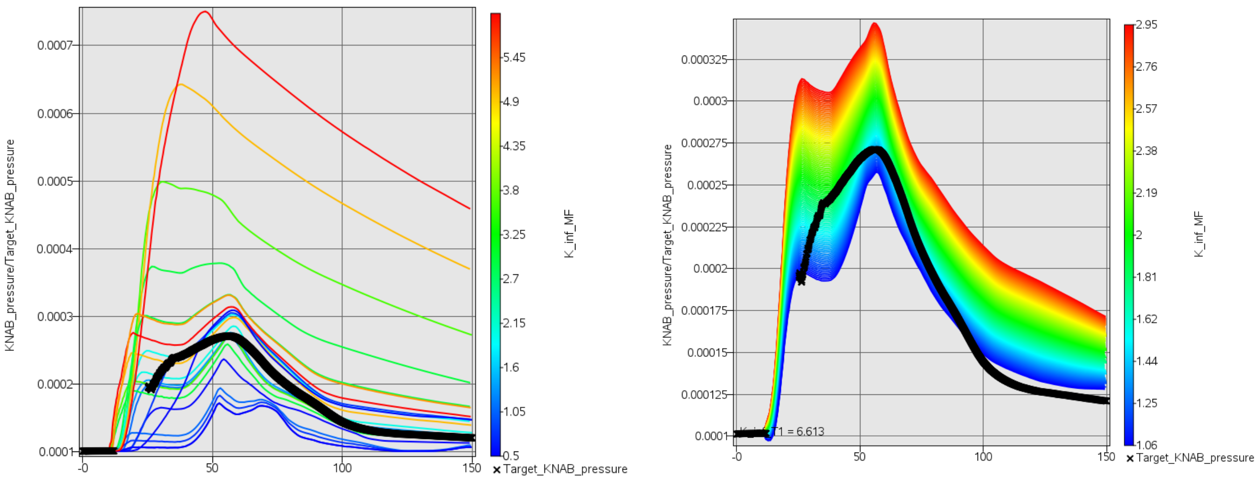

Figure 4.8: KNAB pressure optimization, colors showing simulations with different values on inflator mass flow peak $\dot{m}_{max}$ and target curve presented in black. Simulations without metamodel (left) and results from metamodel (right).

As mention above, no curve for the simplified airbag is the same as the reference. Hence, the curves that gives a pressure as similar to the reference model at the time when the dummy interact with the airbags, i.e. approximately at $t = 40$ milliseconds, is chosen as the optimal curve. The final parameter for the inflators can be seen in Table 4.7. As mentioned before, the trigger time t_0 was not tuned.

The optimized values where used in the one to one test and the pressure curves for the reference, simplified and tuned simplified PAB is shown in Figure 4.9. The plot confirm that the pressure was way too high before the tuning. There are several possible explanations for this result. The main reason is that the PAB in the reference model is folded when the inflator starting pumping in gas. Before the bag is unfolded the volume is very small the pressure becomes very high, i.e. the pressure peak seen in the plot. The simplified PAB is already unfolded from the beginning and is therefore filled with air before the inflator is triggered. Hence, having a simplified inflator that pumping in the same amount of gas in the unfolded airbag as in a folded airbag results in a too high pressure. In short, lowering the mass flow peak in the simplified inflator compensate for all the air that already is inside the simplified bag.

Lastly, Figure 4.10 compares the pressure curves for the reference, simplified and tuned simplified KNAB. The same claims made above for the PAB are valid for the KNAB also since the reference KNAB is folded while the simplified model is unfolded from the start.

Table 4.7: Inflator parameters for PAB and KNAB, before and after optimization. Parameters tuned written in blue.

Part	t_0 **[ms]**	t_1 **[ms]**	t_2 **[ms]**	$\dot{m}_{max}$ **[kg/ms]**
PAB	0	16.2	45	3.76
PAB - Tuned	0	25	35	1.06
KNAB	0	2.15	11.6	5.2
KNAB - Tuned	0	19	28	0.77

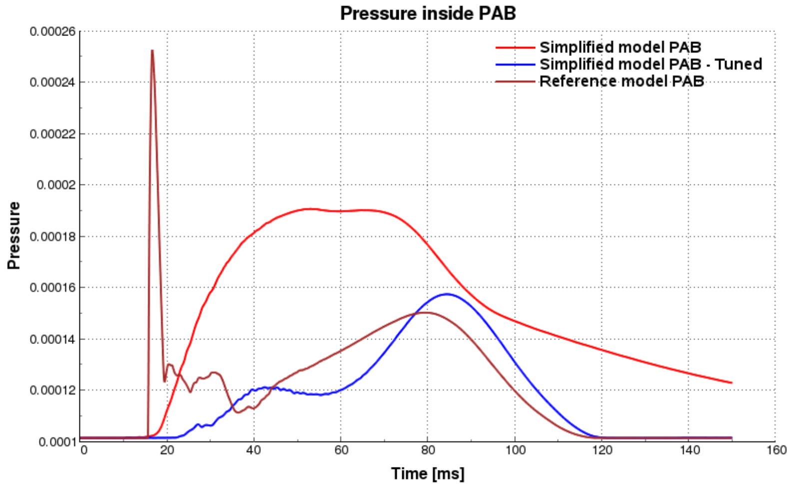

Figure 4.9: Comparison of PAB pressure between reference model, simplified model and tuned simplified model.

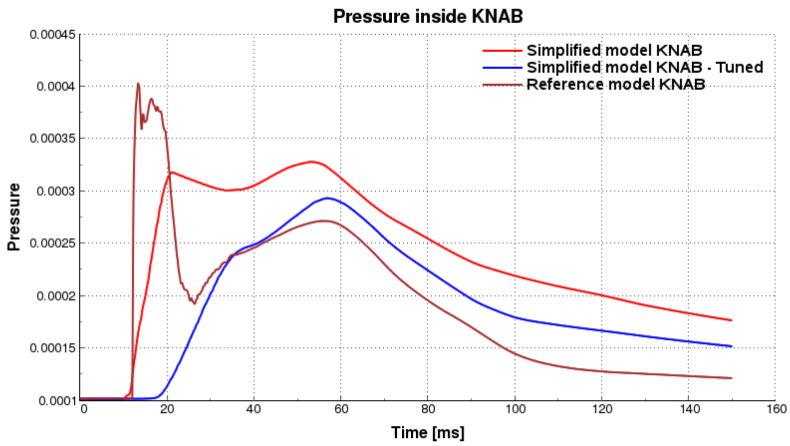

Figure 4.10: Comparison of KNAB pressure between reference model, simplified model and tuned simplified model.

4.3.3 One to one comparison after tuning parameters

The detailed PAB and KNAB in the reference model are replaced with the simplified tuned models. The same simulation and result are extracted as in the one to one test presented above. Table 4.9 compares the summary of the risk indicators before and after tuning of the models. For more comparing risk indicators between the reference and the tuned parts, see Appendix B.

Table 4.8: Risk indicator comparison between reference, simplified and tuned simplified parts.

Model	HIC_{15} [-]	Error	$CCLIP3m$ [g]	Error	Cd [mm]	Error
Reference	425	-	51.1	-	18.6	-
Simplified PAB	848	100%	61.5	20%	38.9	109%
Simplified PAB - Tuned	880	107%	61.2	20%	13.1	30%
Simplified KNAB	491	16%	56.3	10%	20.5	10%
Simplified KNAB - Tuned	460	8%	58.5	14%	20.1	8%

Reference model with tuned simplified PAB.
The kinematic comparison of the tuned PAB is shown in Figure 4.11. As the figure shows, there is a considerable difference in the behavior of the dummy with the tuned PAB compared to before. The dummy is not bouncing back as much as it did in the first test. This correlates to the lower chest deflection seen in Table 4.1. Further, the HIC value is not lowered but increased which is an unexpected result. The maximum chest acceleration decreased by a small amount.

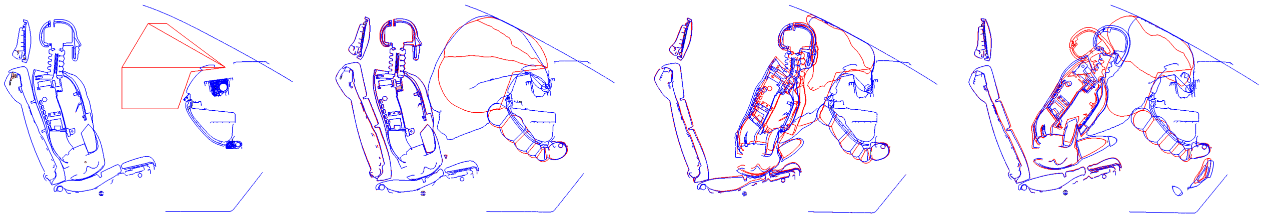

Figure 4.11: Dummy kinematic comparison between reference PAB (blue) and tuned simplified PAB (red). Side view with slice cut in the middle of the dummy. Time steps: 0 ms, 40 ms, 80 ms and 120 ms.

Reference model with tuned simplified KNAB.
The kinematic comparison of the tuned KNAB is presented in Figure 4.12. By studying the third frame in the figure, it is possible to see that the dummy has penetrated the airbag more compared to the model before tuning. As for the PAB, it is because of that the pressure in the bag is lower after tuning. It can be seen from the data in Table 4.9 that the error of the HIC and chest deflection are decreased but the maximum chest acceleration is increasing. Overall, the results from the tuned PAB and KNAB indicates that the optimization of the models made them behave more like the reference model in terms of kinematics.

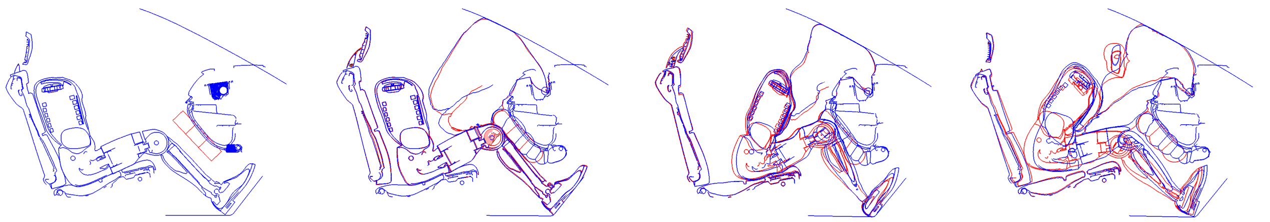

Figure 4.12: Dummy kinematic comparison between reference KNAB (blue) and tuned simplified KNAB (red). Side view with slice cut in the middle of the dummy knee. Time steps: 0 ms, 40 ms, 80 ms and 120 ms.

4.3.4 Validation of complete final model

The results of the simulations performed with the final model with all tuned parts included are shown in Figure 4.13 and Table 4.9. The figure visualizes the difference in kinematics between the reference and the final simplified model. It is clear that the simplified model is deviating from the reference. This fact is also proven by the big difference in risk indicators presented in the table. Interestingly, the maximum chest acceleration is higher than the reference, at the same time the maximum chest deflection is much lower. This may be explained by the fact that the dummy have only one measuring point for chest compression located at the mid sternum. If the load is not located at that point the chest compression will be low. In the simplified model the upper part of the chest, the throat and the head are the main parts in contact with the PAB. Hence, the chest may deflect less compared to the reference model where the whole chest is in contact with the PAB.

Table 4.9: Risk indicator comparison between reference and final simplified model.

Model	HIC_{15} [-]	**Error**	$CCLIP3m$ [g]	**Error**	Cd [mm]	**Error**
Reference	425	-	51.1	-	18.6	-
Final Simplified model	608	43%	55.4	8%	8.1	56%

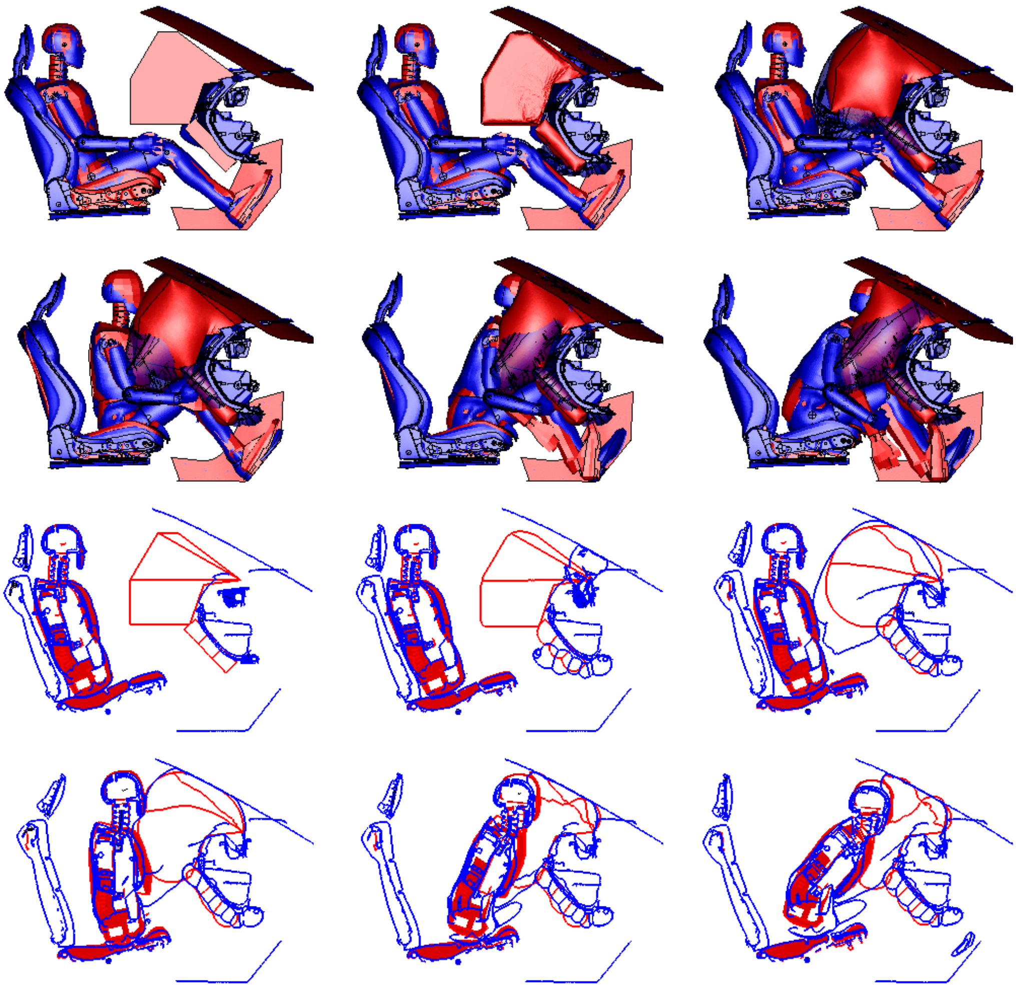

Figure 4.13: Dummy kinematic comparison between reference model (blue) and final simplified model (red). Side view without and with slice cut in the middle of the dummy. Time steps: 0 ms, 20 ms, 40 ms, 60 ms, 80 ms and 100 ms.

However, these findings are rather disappointing, and indicates that the exact numbers given from the simplified model cannot be directly compared to the reference model. Lastly, the aim was to develop a less computer costly model. The simplified model simulates a 150 millisecond long simulation on 240 cores in 35 minutes compared to the reference model which takes 8 hours to run with the same setting. Hence, the simplified model is almost 14 times faster compared to the reference.

4.4 Stochastic simulation

First, the robustness test of the model did not result in any simulation with error termination. Therefore, no changes were made of the parameter setup and out of the 150 simulations ran with the defined input in section 4.1, all 150 went through with normal termination. Further, the result from the stochastic simulation is divided into two sections, one presenting the resulting responses with corresponding statistics and plots, and the second part focusing on the histories.

4.4.1 Resulting responses from the stochastic simulation

From each simulation, the corresponding responses defined in section 4.2 are computed. After all simulations are run, statistical data is extracted and plotted, e.g. in scatter plots. A linear correlation matrix of all the responses of the parameter study is presented in Figure 4.14. The correlation number varies from -1 to $+1$, where ± 1 indicates perfect correlation and 0 no correlation. Furthermore, Table 4.10 provides the mean and standard deviation of each response. Every combination of parameters cannot be presented in detail. Hence, a few interesting results for each input parameter and some combinations of output parameters will be discussed further.

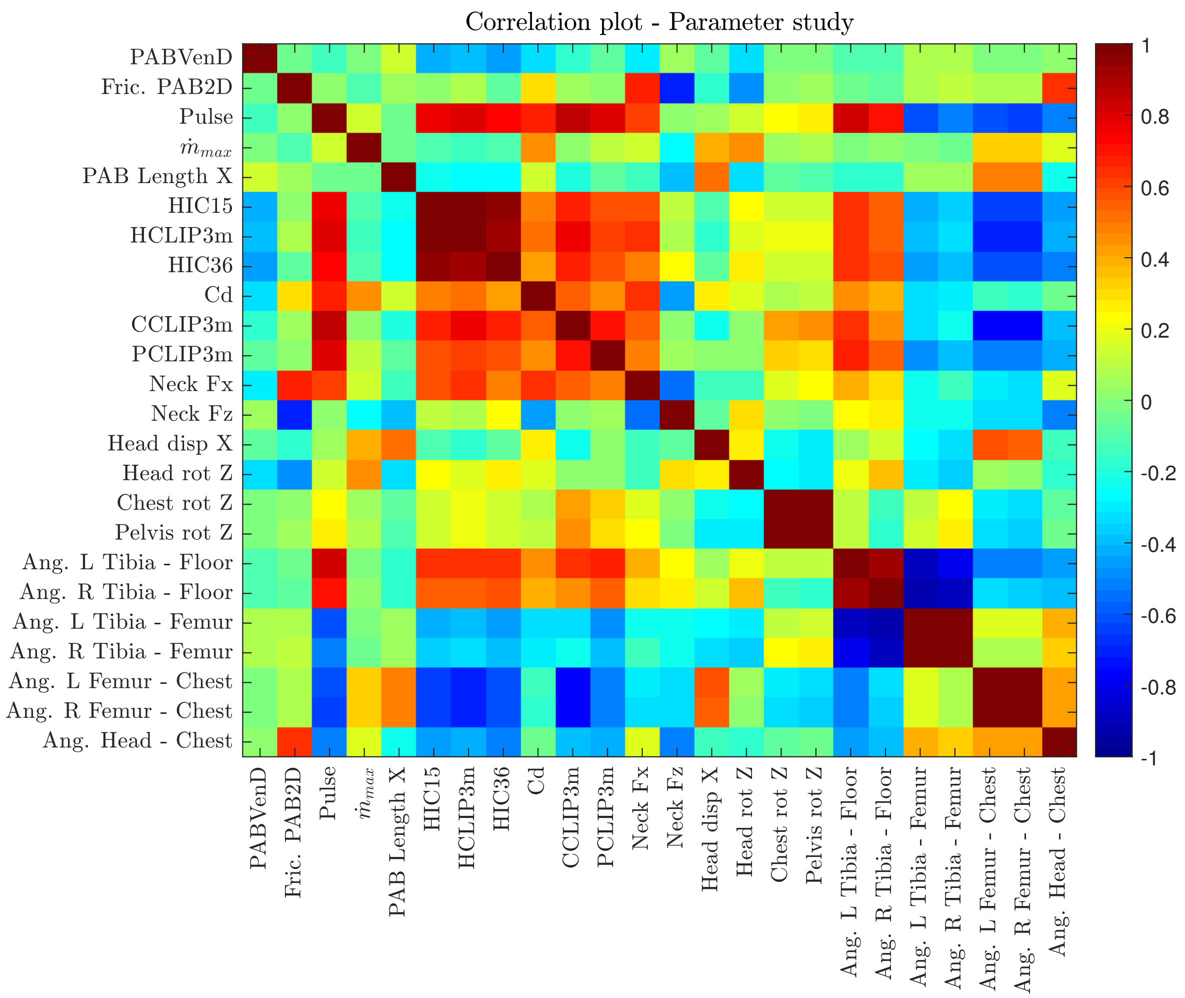

Figure 4.14: Linear correlation matrix of all parameters in parameter study.

Table 4.10: Statistical distribution of responses from parameter study.

Response	Max/min	Unit	Mean	Standard Deviation
HIC_{15}	Max	[-]	554	63.7
HCLIP3m	Max	[g]	72.3	3.79
HIC_{36}	Max	[-]	720	73.6
Cd	Max	[mm]	6.96	0.768
CCLIP3m	Max	[g]	49.8	5.75
PCLIP3m	Max	[g]	37.8	2.99
Neck F_x	Max	[kN]	2.16	0.154
Neck F_z	Max	[kN]	0.944	0.162
Head disp X	Min	[mm]	-987	28.6
Head rot Z	Max(abs)	[deg]	14.3	2.61
Chest rot Z	Max(abs)	[deg]	1.37	0.57
Pelvis rot Z	Max(abs)	[deg]	1.26	0.48
Ang. L Tibia - Floor	Max	[deg]	21.9	1.63
Ang. R Tibia - Floor	Max	[deg]	21.3	1.81
Ang. L Tibia - Femur	Min	[deg]	-21.0	1.87
Ang. R Tibia - Femur	Min	[deg]	-20.5	2.00
Ang. L Femur - Chest	Min	[deg]	-44.7	1.70
Ang. R Femur - Chest	Min	[deg]	-44.7	1.72
Ang. Head - Chest	Min	[deg]	-20.7	1.59

4.4.2 Results visualized in scatter plots

The result of all the simulated points appears as grey dots in the scatter plots. A linear fitted line is also plotted and the coefficient of determination R^2 showing how well the data is fitted to the curve. Moreover, the nominal run is presented in red color.

PAB vent diameter.
The diameter of the PAB ventilation hole is not controlling any of the result parameters to a great extent. However, the data shows a weak relationship between an increasing diameter of the PAB ventilation hole results in decreasing values of the risk indicators, i.e. negative correlation coefficient. Figure 4.15 presents the scatter plot of HIC_{15} and CCLIP3m versus PAB ventilation hole diameter. By comparing the two plots the PAB vent diameter has a higher influence on the acceleration of the head compared to the pelvis. Moreover, closer inspection of the correlation matrix shows that it not seems to be any correlation between any rotation angle and change in PAB ventilation diameter, i.e. green squares in the linear correlation matrix shown before.

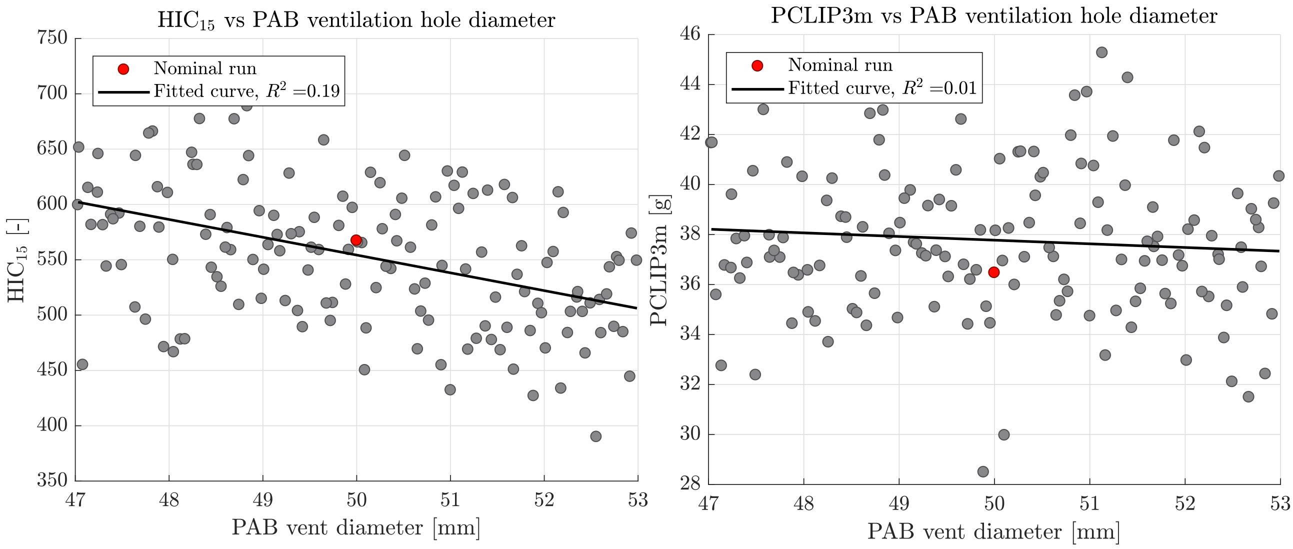

Figure 4.15: Scatter plot of HIC_{15} vs PAB vent diameter (left) and CCLIP3m vs PAB vent diameter (right).

PAB - Dummy friction.
It is a significant correlation between the force in the neck and the friction between the PAB and dummy. This is an expected outcome since a higher friction prevents the head from sliding on the airbag surface and more force is transferred trough the neck, see Figure 4.16 for scatter plot. Interestingly, an increase of friction between the dummy and PAB lead to a decrease in angle between head and chest, in other words, the neck is less bent. Further, no correlation between the friction and the head, chest or pelvis acceleration is seen.

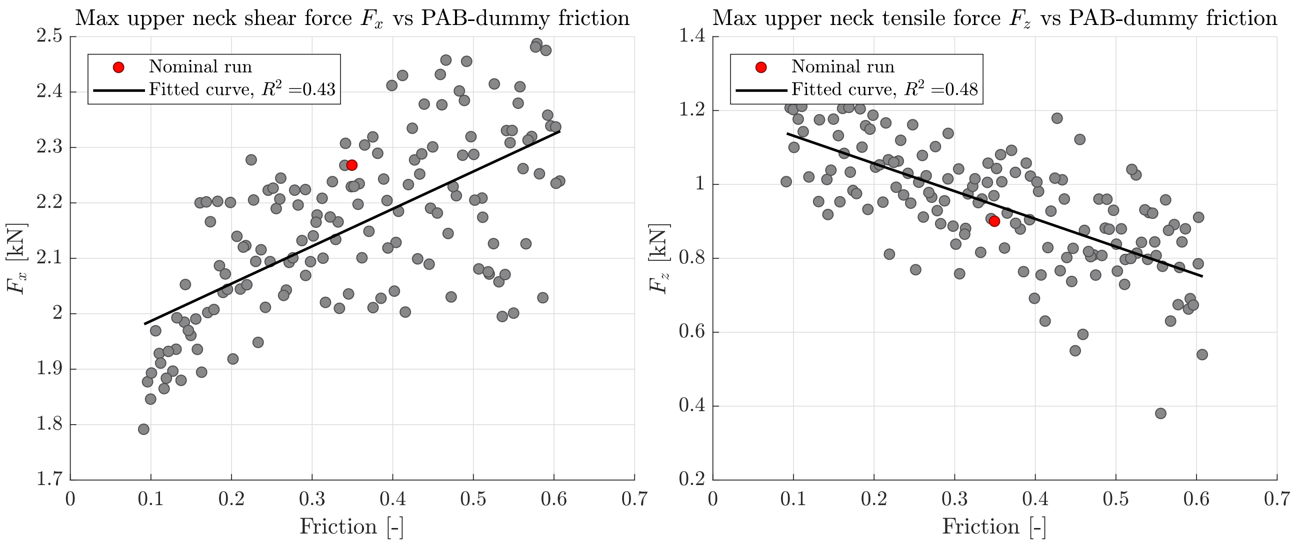

Figure 4.16: Scatter plot of max upper neck shear force F_x (left) ad tensile force F_z (right) vs PAB - dummy friction.

Pulse.
From the data in Figure 4.14, it is apparent that the pulse has a large impact on the response. A pulse resulting in a higher VPI results in higher values of the risk indicators, e.g. HIC value or maximum chest deflection. These trends correlates well to internal studies done at VCC. Interestingly, a higher VPI does not correlate to higher upper neck tensile forces or that the head goes further forward in the crash, i.e. the squares in the correlation matrix is green for these parameters. The difference in the scatter plots of a good correlation versus no correlation can be seen in Figure 4.17 showing HIC_{15} versus VPI and maximum upper neck tensile force F_z versus VPI. Moreover, the measured angles around the Y axis correlates well to the pulse, i.e. the positive increasing angles increase more when the VPI is increased and the negative decreasing angles decrease more when the VPI is increased. Figure 4.18 shows both the angle between the tibia and floor, and between femur and chest versus the VPI.

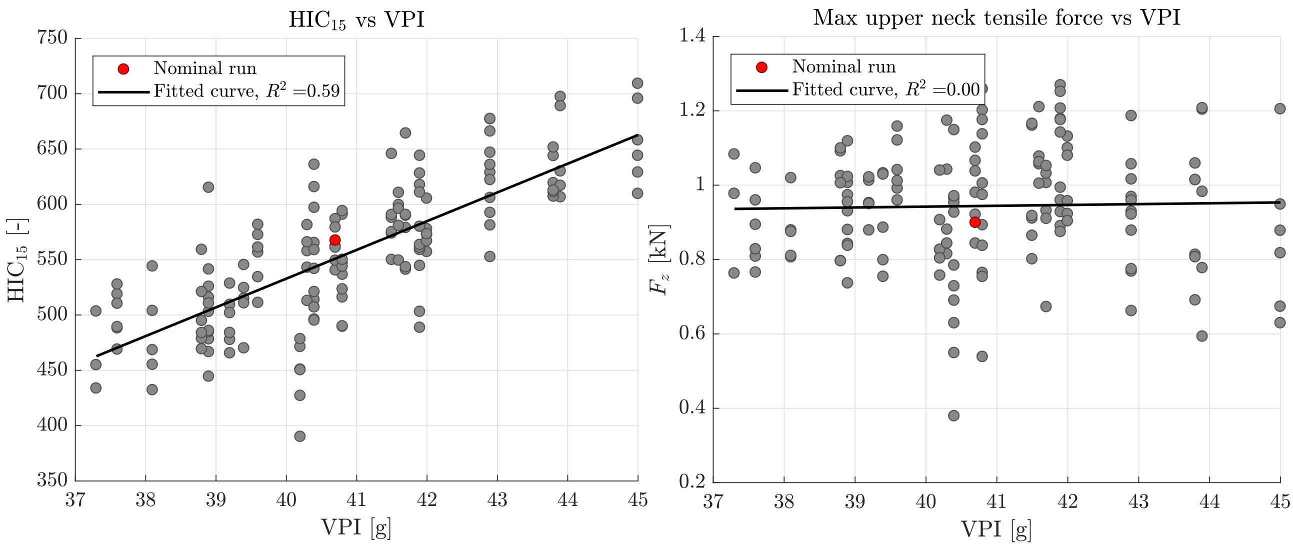

Figure 4.17: Scatter plot of HIC_{15} vs VPI (left) and upper neck tensile force F_z vs VPI (right).

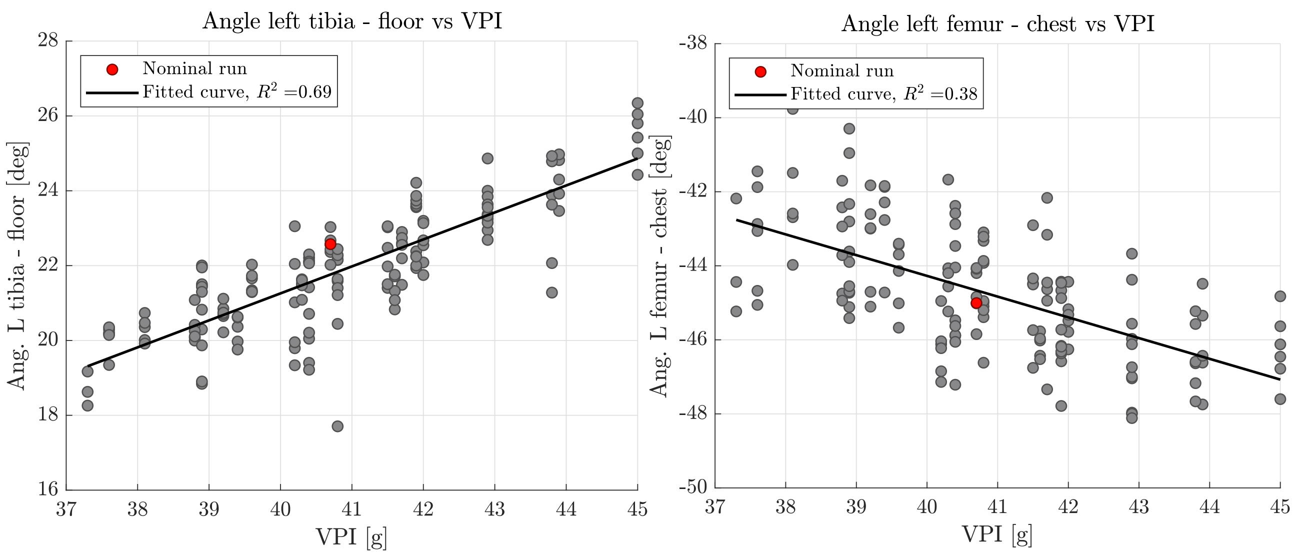

Figure 4.18: Scatter plot of angle between left tibia and floor vs VPI (left) and left femur and chest vs VPI (right).

PAB inflator mass flow peak, $\dot{m}_{max}$.
Figure 4.19 shows the comparison of max chest deflection Cd and chest acceleration CCLIP3m versus the PAB inflator mass flow peak value $\dot{m}_{max}$. The Cd has a positive correlation with the mass flow peak, which is not surprising, since a higher mass flow leads to higher pressure in the airbag. More interestingly is the fact that the max accelerating of the chest does not seem to be affected. Further, the inflator mass flow peak does not seem to significant influence the kinematics of the dummy. The highest correlation coefficient is found for the angle between the femur and chest. It makes sense since a higher mass flow results in higher pressure, hence the chest does not sink as deep into the bag.

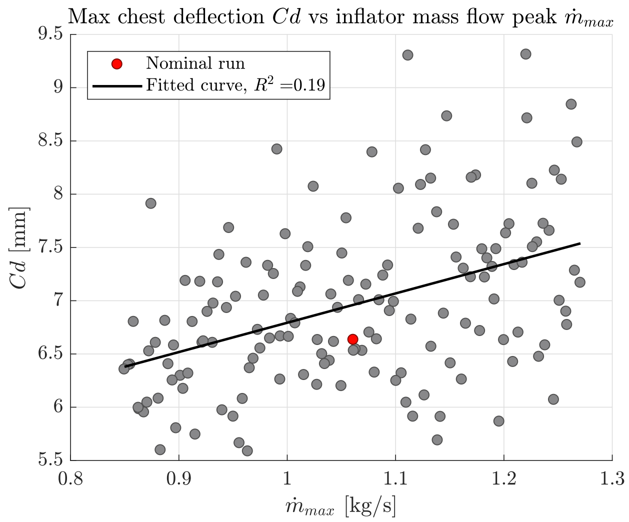

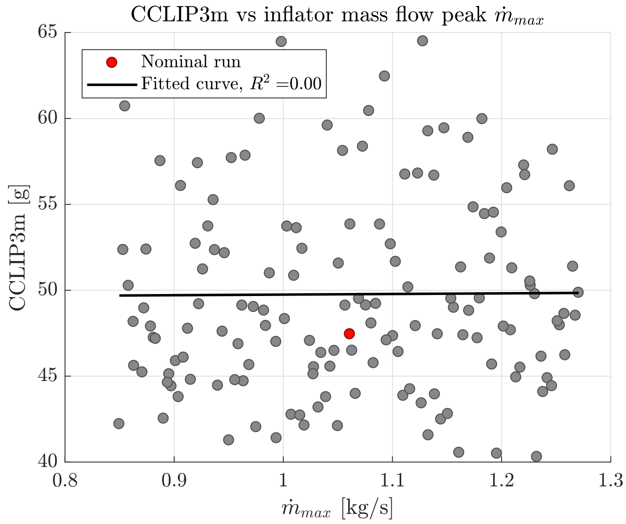

Figure 4.19: Scatter plot of max chest deflection Cd vs $\dot{m}_{max}$ (left) and CCLIP3m vs $\dot{m}_{max}$ (right).

PAB length in X-direction.
The HIC_{15} and max chest deflection Cd is plotted versus the PAB length in X-direction in Figure 4.20. The result obtained from the scatter plot is that the HIC_{15} value seems to be lowered if the PAB length is increased, i.e. if the dummy is captured by the airbag earlier. However, it comes with the cost of a higher maximum chest deflection. The correlation between the kinematics are similar to the increase of mass flow. A longer airbag results in the chest being less tilted forward.

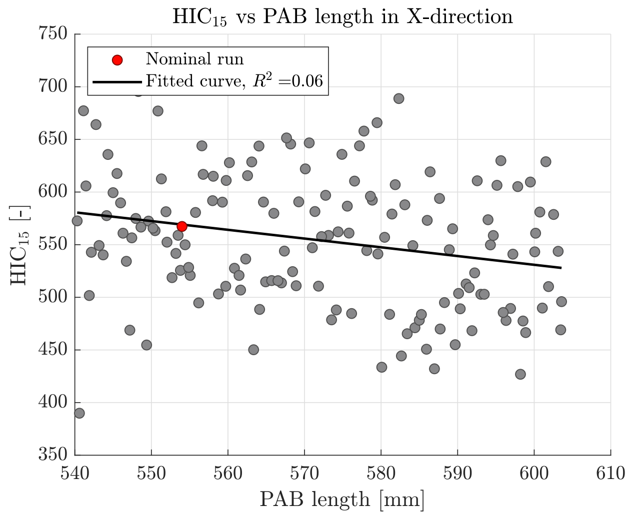

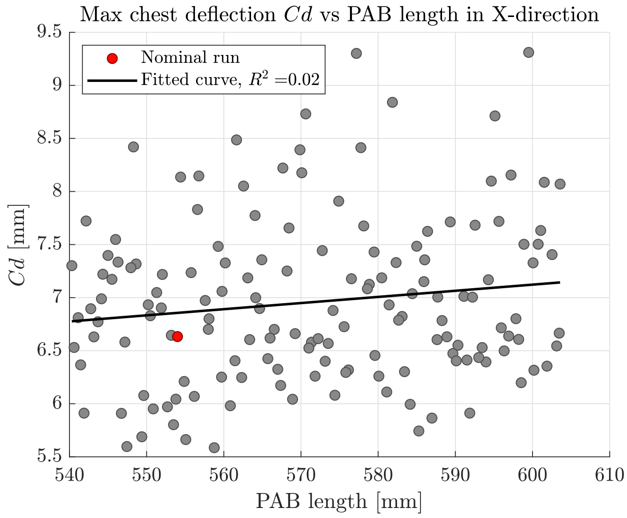

Figure 4.20: Scatter plot of HIC_{15} vs PAB length in X-direction (left) and max chest deflection Cd vs PAB length in X-direction (right).

Response versus response.
It is not only interesting to analyze input parameters against responses; it is also possible to see the how two parameters co-variate. As an example, Figure 4.21 presents the scatter plot of HIC_{36} versus CCLIP3m. This type of plots exposes how much the output is spread by the defined input parameter distributions. By changing some input parameters, the risk indicators seem to vary a lot. Furthermore, it is also possible to draw conclusions on relationships between risk indicators and kinematics of the dummy. By looking at the correlation between them, some trends of what a good kinematic behavior is can be found. As an example, Figure 4.22 compares the angle between the right femur and chest with the CCLIP3m. The plot indicates that a less forward rotated chest is beneficial in terms of low chest acceleration. Lastly, it is also possible to see the relation between dummy kinematics. The angle between the femur and chest and the angle between the head and chest is plotted in Figure 4.22. A lower angle between the femur bone and the chest appear to result in a lower angle between the head and chest, i.e. a less bend neck.

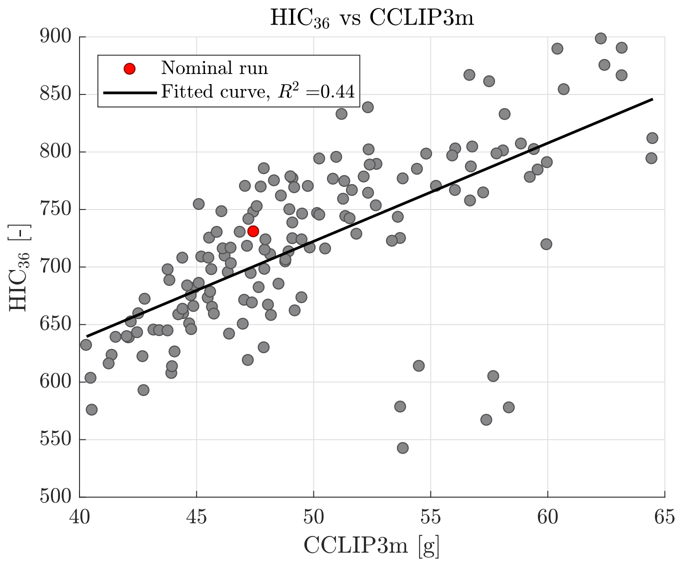

Figure 4.21: Scatter plot of HIC36 vs CCLIP3m.

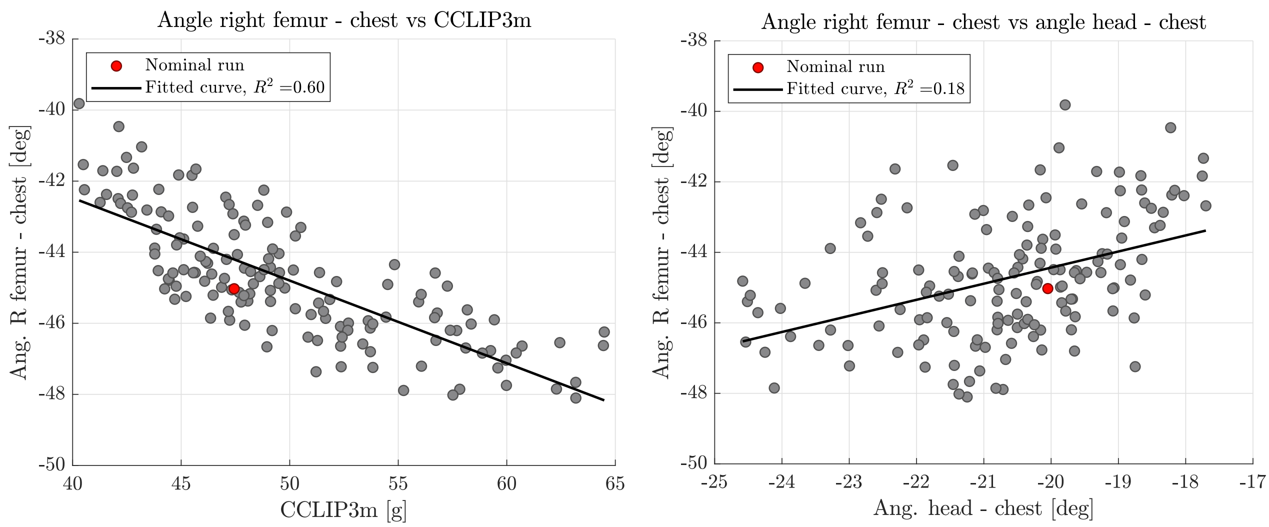

Figure 4.22: Scatter plot of angle between right femur and chest vs CCLIP3m (left) and vs angle between head and chest (right).

To sum up, the scatter plots visualize the big spread of all responses and that all responses are affected by the change of input parameters. Moreover, the scatter plots indicate that correlation occur between some parameters and some not. In general, the system response is highly sensitive.

4.4.3 Sensitivity of input parameters

The global sensitivity analysis is performed in the parameter study. The sensitivity plots show how sensitive the responses are to each input parameter. Figure 4.23 displays the global sensitivities for the head, chest and pelvis acceleration, chest deflection, upper neck F_x and F_z force and the head X displacement. Each bar represents the contribution of a variable to the variance of the respective response which is presented in different colors. The values are normalized such that the sum of all displayed values is 100%. The pulse has the highest influence on the accelerations and chest deflection. In contrast, the sensitivities for the minimum head displacement in X-direction is not sensitive to the pulse at all. This is more clear in Figure 4.24 where the sensitivity plot only for the minimum head displacement in X direction is shown. Interestingly, the head displacement in X-direction is mainly affected by the airbag properties.

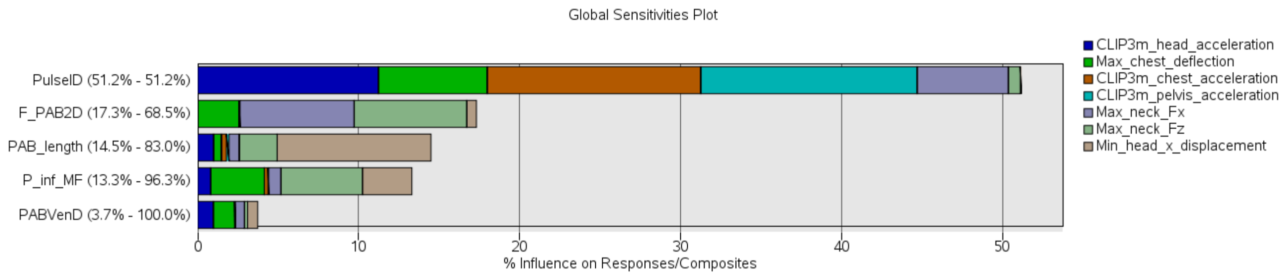

Figure 4.23: Sorted global sensitivities of the responses.

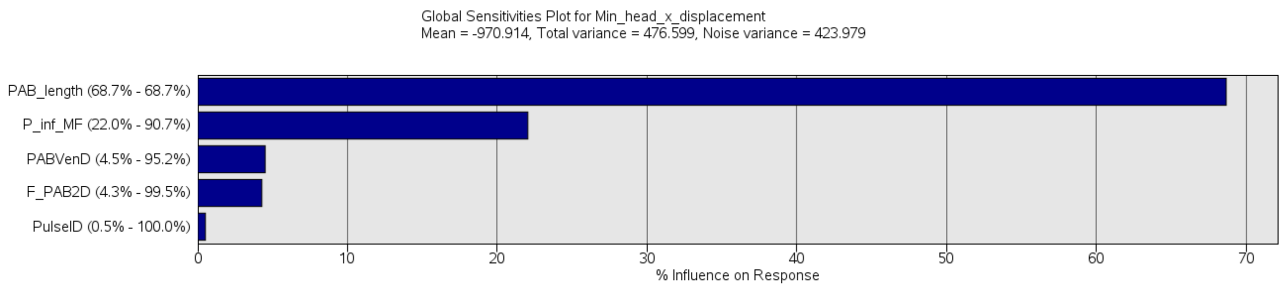

Figure 4.24: Sorted global sensitivities of the minimum head displacement in X direction.

4.4.4 Results visualized in history curves

The history curves are based on time data or cross plots obtained from simulations. Compared to scatter plots, the history plots do not only show spread from one value, it shows the spread over the whole time sequence of a simulation. As an example, Figure 4.25 shows the history of the head acceleration for all of the 150 simulations. The history plots are mainly used as a tool to see the spread but it can of course also be used to see results from a specific run since every curve is connected to a simulation. Another example is the airbag pressure presented in Figure 4.26 showing how the pressure in the PAB is spread for the varying input parameters.

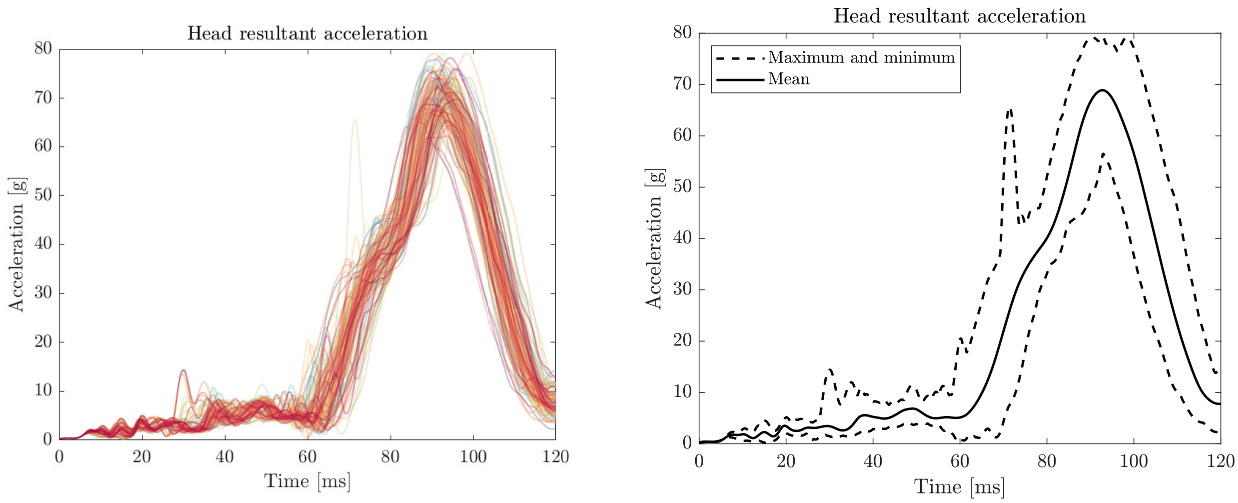

Figure 4.25: History plot of head acceleration vs time.

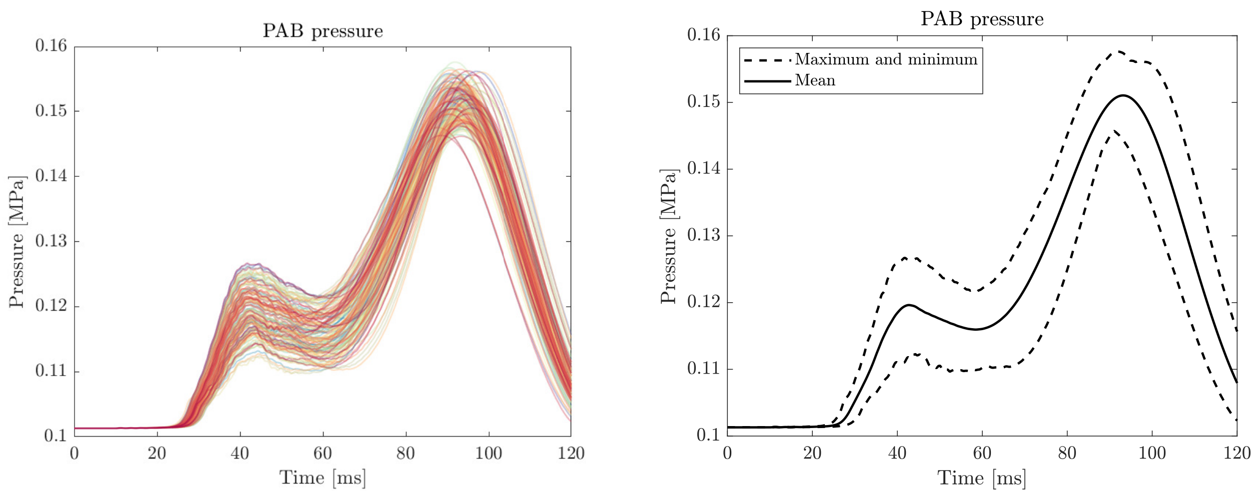

Figure 4.26: History plot of airbag pressure vs time.

The history plots are probably the most efficient tool to understand the kinematic of the dummy, i.e. plot the displacement and change in angles over time. Figure 4.27 shows all the rotations around the Y axis. It can be seen from the graphs that the dummy does not interact with the floor, KNAB or PAB before 40 milliseconds since there are no change in angles. However, after 40 milliseconds the angle between the tibia bone and the floor is increasing since the feet comes in contact with the floor and the knees are not stopped by the KNAB yet. Secondly, the angle between the tibia and femur bone is decreased since the pelvis is moving forward at the same time as the feet is stopped by the floor. Thirdly, the angle between the femur bone and the chest is decreasing when the knees are stopped by the KNAB and the upper chest and head drops into the PAB. Lastly, the angle between the head and chest is shifted in time since it is the last part getting into any contact. The angle is decreasing, i.e. the neck is bent backwards, due to the chest going deeper into the PAB.

The dummy interactions with different parts are also visualized in Figure 4.28 where the displacement of the head, chest and pelvis are plotted. It is clear to see that the head, chest and pelvis are stopped in different sequences resulting in the rotations mentioned above. Further, the pelvis and chest are displaced more in Z compared to the head which shows that the chest has been tilted forward and the neck is most likely bent backwards. Lastly, Figure 4.29 presents the rotations around Z. The only part significantly rotating around this axis is the head, the chest and pelvis does not rotate much which is expected in this load case.

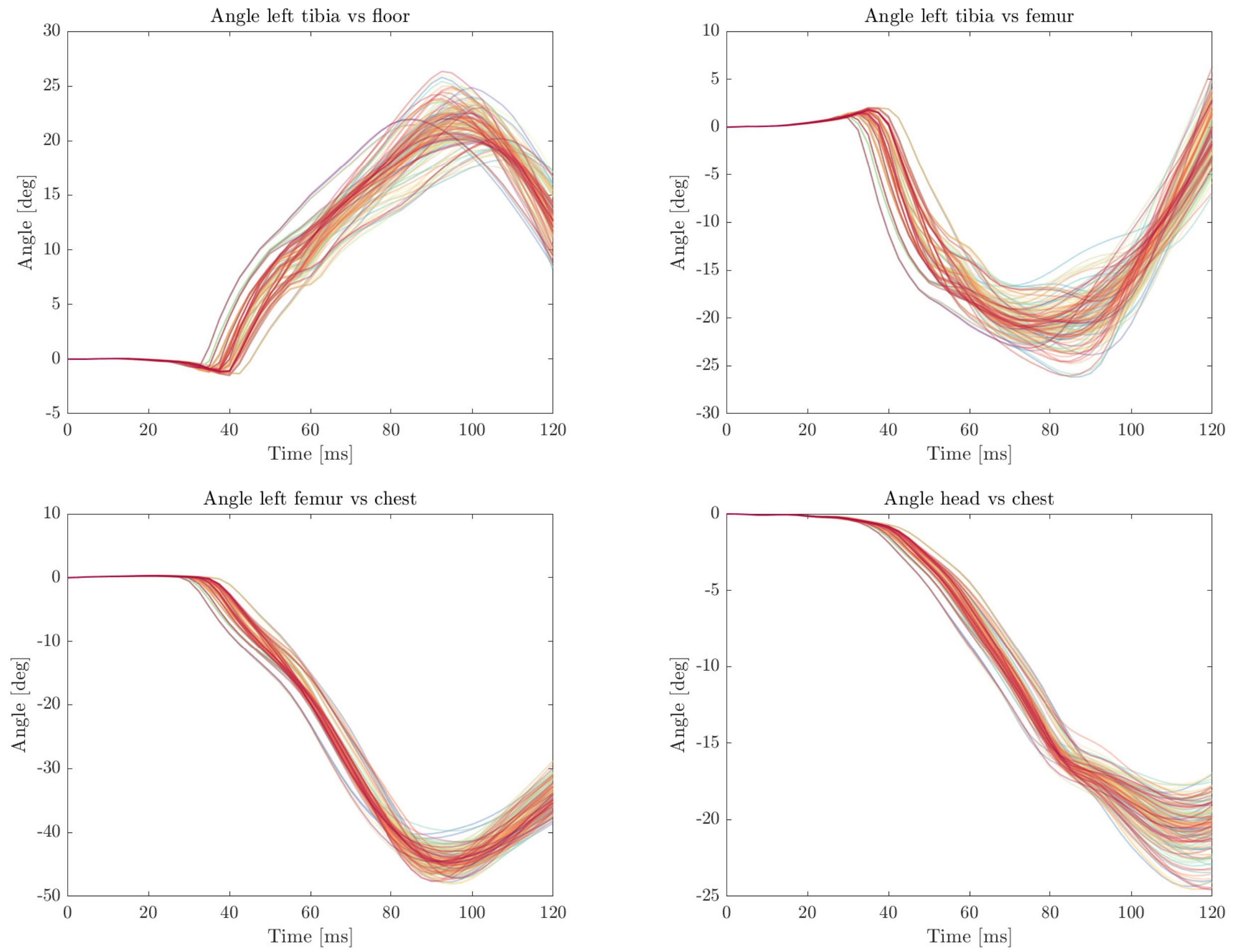

Figure 4.27: History plot of angle L Tibia - Floor (upper left), L Tibia - Femur (upper right), L Femur - Chest (lower left) and Head - Chest (lower right).

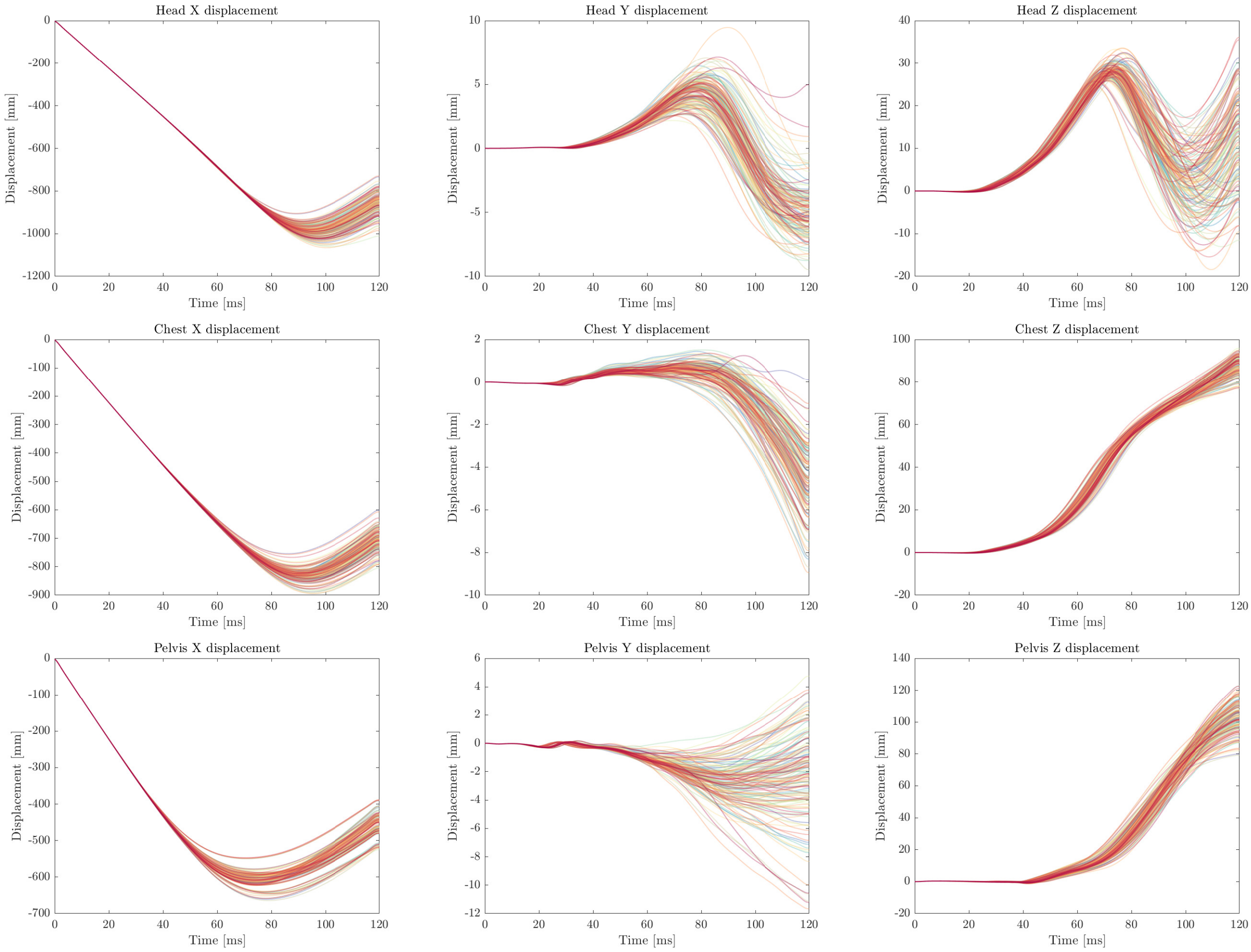

Figure 4.28: The displacement of head (top), chest (middle) and pelvis (lower) in X, Y and Z direction respectively.

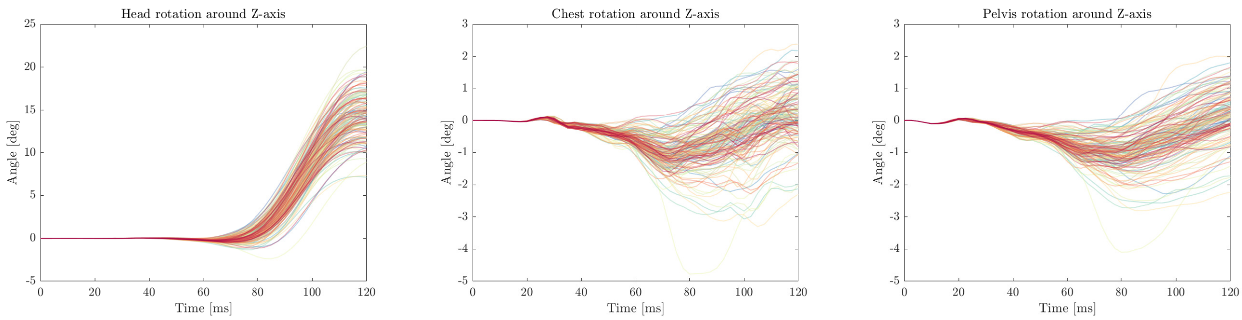

Figure 4.29: The rotation of head (left), chest (centre) and pelvis (right) around the Z axis.

4.4.5 Parameter study summary

In summary, correlation analysis, scatter plots and sensitivity analysis has been presented based on responses of the stochastic simulations. Further, history curves based on time data were shown to visualize the spread of outputs over time.

The strongest correlation and effect was found between the Pulse and the injury criteria based on acceleration. History plots of the kinematics can be helpful to see the spread in dummy kinematics in the stochastic simulations. It can also be used to understand when different parts are interacting with the surroundings, e.g. the offset of the pelvis, chest and head displacement in X-direction.

5 | Discussion

In this chapter, the methods used, and the results gathered will be discussed with focus on the fulfillment of the project goals, expected and unexpected outcome and sources of uncertainties. First, the selection of input and output parameters are discussed. Secondly, the development and validation of the simplified model. At last, the findings from the stochastic simulations are commented.

5.1 Selection of input parameters

An initial objective in the project was to identify relevant input parameters that affected the behavior of the system. The list gathered from literature, physical tests and simulation became long and it was clear that several parameters affect the system in one way or another. Moreover, some parameters even affect each other which makes the system even more complex. Very little was found in the literature on how to choose which parameters to vary or how to decide on the statistical distribution. It was also shown in the project that it is hard to gather the right statistical information. The car manufactures main focus lies with the nominal values of the parameters instead of the statistical distribution. Thus, the input parameters had to be chosen with no strong foundations.

It is critical to choose the right parameters because if too too many parameters are chosen, the combination of them will exponentially grow the amount of runs needed. The current study indicates that several parameters can have different distributions depending on the parameter type, i.e. *production*, *design* or *real life*. Hence, it is important to state the objective of the study in order to decide which type of parameters to study. If the objective is to get five stars in a crash test, production parameters with the manufacturing tolerances should be used to make sure the score is achieved. If the objective is to get the best possible protection for occupants in real life crashes, the variation from real life crashes should be used. A proposed method to go further with the input parameter is to perform a Design of Experiment with all input parameters in the simplified environment in order to see which parameter has the highest impact on the system and use these for the stochastic simulation.

In this project, five parameters were chosen for the stochastic simulations. First, the parameter *PAB length in X-direction* was used as a design parameter with uniform distribution. The parameter was chosen to get at least one design parameter that affects the geometry. Thus, the morphing tool in ANSA was used and connected together with LS-OPT. The mesh was not reconstructed after each morphing, but the mesh was checked afterwards and judged to be good. Further, the lengths were set such that the airbag did not get any cross-edges with the surrounding parts. Other parts could have been used for the same purpose mentioned above, but the PAB length in X-direction is an interesting parameter to study since it show the influence of an earlier contact between the PAB and dummy without changing the seating position.

The *PAB inflator mass flow peak* parameter was set to the tuned value $\pm 20\%$ to reflect a tunable range for the inflator. Since the simplified PAB is unfolded from the beginning, the change in mass flow does not affect the deployment or positioning of the bag. Instead, it mainly affect the pressure within the bag which could be achieved by changing other parameters instead, for example the temperature. Compared to the temperature, the inflator mass flow is a tunable parameter and was therefore selected as input.

The *diameter of the PAB ventilation hole* was used as an example of a production parameter. The hole of the physical airbag is cut with a machine with a certain tolerance. Even if the machine is highly accurate, a spread will exist. The parameter was given a normal distribution with the mean value 50 millimetre which was estimated as a standard size by engineers at VCC. There was no time to get information about the exact spread measured in the manufacturing process. Hence, the standard deviation was set to 1 millimetre which is a tolerance used. The reasons why the parameter was used are first that it is a parameter that is possible to readjust in late phases in the development process which makes it valuable. Secondly, the ventilation hole is the only parameter affecting the gas leaking out of the airbag since the woven fabric used in the airbag model was coated and the influence of changing it is of interest.

According to the safety engineers at VCC, the *crash pulse* highly influences the consequences of a car crash. Therefore, it was chosen as one of the important input parameters to include in the simulations. Meetings were held with an experienced CAE engineer at Volvo Cars Safety Centre to find a way to quantify the pulse curve to a statistical distribution. It does not exist any trivial way to do this since the crash pulse is a curve and not a single value. The proposed method was to use the VPI to measure the severity of the pulse. To get a spread of the VPI, 28 different pulse shapes were defined. The VPI varied from 37.3 g to 45.6 g which is a broad spread compared to the distribution of the other input parameters. Knowing the outcome of the simulations, one can argue that the spread was too wide and the crash pulse too influential compared to the other parameters

In reviewing the literature, no data was found on using the VPI as an input parameter for the pulse variation. However, Iraeus [5] used eigenvalues to approach the variation of the crash pulse. Using the VPI as input can however be a little misleading since it is computed similar to the risk indicators based on acceleration, but with an extremely simplified vehicle model. Hence, one can motivate that the VPI is a form of an output instead of an input to the system. Further, in comparison to the other input parameters, the pulse is changed very much and using two different pulse shapes correspond to using two very different cars. Therefore, input parameters of the restraint system can have too little influence compare to changing the car crash structure. Seen from this angle, an alternative approach more like Iraeus could suit better as input to the stochastic simulation. It would make it possible to control the shape of the pulse curve which was not possible in this study.

The *friction between the PAB and dummy* was selected as a real life parameter. The friction coefficient between the PAB and a crash test dummy can be even more spread out than what is used in this study. However, it is impossible to determine one exact friction coefficient between every occupant and the PAB due to different clothing materials, hair or other real life factors. To see if the friction has a high influence on the output, the friction coefficient was approximated to a uniform distribution parameter between 0.1 and 0.6. A more exact distribution could be achieved by doing a study of friction coefficients between different fabrics used in airbags and clothes. Further, one coefficient can be used for the head and another for the torso.

In general, the five parameters used in this thesis were chosen to test the method with different approaches and statistical distributions representing the three types of input parameters. No parameters in the simplified KNAB were varied to keep the number of simulations feasible within the time frame.

5.2 Selection of output parameters

The FAST50 simplified dummy used in the project has not been tested or validated at VCC. After investigation of the dummy in this study, it stands clear that it is limited in the number of sensors available for measuring. The results from the comparison with the detailed HIII 50th dummy showed errors of the risk indicators over 10%. These errors may be explained by the fact that the FAST50 dummy is stiffer due to the simpler material models and that larger finite elements are used. Hence, using the FAST50 dummy, adds more uncertainties to the correlation and the results deviates further away from both physical testing with the common used HIII 50th dummy and "real life" scatter. In other words, the FAST50 dummy is a simplification of the virtual HIII 50th dummy which is a model of a mechanical model of a human. In total, this may lead to worse correlation not only in risk injury criteria, but also in the different kinematics.

The limitations of risk injury criteria possible to measure with the FAST50 dummy were not only due to that less instruments are included in the dummy. It was also affected by the fact that LS-OPT has not included that dummy model in its library. Hence, all equations must be defined by hand and the output needed for some of the values could not be extracted by LS-OPT, for example the upper neck moment M_y that is used for the neck injury criteria. Further, only accelerations of parts affected by interaction with the simplified parameters parts were included. In this study, the focus was set to the head, chest and pelvis. In short, the need for studies on which risk injury criteria that is best to use in stochastic simulations still exists and should be performed with a more detailed dummy.

The present study was designed to determine a way to measure the influence of varying input parameters in terms of kinematics of the dummy. It was found that the kinematic for a dummy in this specific load case follows a certain pattern. The dummy rotates around different joints and the rotation depends on the interaction with the seat, floor, KNAB and PAB. Due to that all parts in the dummy are connected, a movement of one part is transferred to another part. Hence only a few measures had to be made to capture the most important movements. Rotations in the YZ plane were excluded since the used load case did not result in any significant rotation in that plane. However, if a side impact was studied, the main rotations would be found in there. The feet and arms were placed in standard positions and were not moved between simulations. Hence, rotation of these parts were not included as output. Instead rotations in the knee-joint, hip-joint and pivot joint in neck were used. Lastly, the trajectories of the head, chest and pelvis were used as output to be able to follow the displacement of the body parts over time.

Interestingly, by knowing the initial position of the dummy, one can easily understand how the dummy has been moving during the impact by looking at the graphs. The way of measuring angles and displacements could be used if a certain kinematic behavior wants to be achieved, e.g. no head rotation or boundaries in maximum head X displacements. Similar measurements were found in the literature when pre-crash maneuvers where studied. Thus, the kinematic output can be used as a tool for that as well.

Furthermore, no big differences were seen between the angles measured with the left or right leg. This is logical since the dummy is symmetric and both the left and right side were positioned the same way. Also because the interaction between the legs and the KNAB was similar since. This would be different with an angled instrument panel and therefore an angled KNAB. Besides, the pulse was applied in X direction only. Hence, an average between left and right could be used as output to decrease the amount of data.

5.3 Development and validation of simplified frontal passenger vehicle FE model

The key to making a trustworthy simplified vehicle model is validation. One unexpected finding was that the simplified PAB resulted in a very different HIC15 value compared to the reference model, even if the pressure curve was close to the reference. More interestingly was the fact that the HIC15 value increased after tuning the parameters, although the kinematic behavior of the dummy became much more like the reference. This finding was unexpected and suggests that the shape of the bag, e.g. the angle between the dummy and interaction area of the bag, has more influence than what was believed before the study. Thus, the shape must be prioritized when simplifying the airbags so the base shape is closer to the one in the reference model.

Another drawback seen with the simplified PAB was that having an unfolded bag from the beginning, prevents the possibility for the bag to unfold into the lower part of the chest and abdomen. Creating a boxy lower part on simplified model led to a too early contact with legs and arms. Hence, the main contact between the PAB and the dummy occurred at the upper chest and head. Whereas, the reference PAB unfolds over the instrument panel all the way down into the lap of of the dummy. Further, the fact that the simplified PAB is already unfolded from the beginning results in that a different inflator compared to the reference model had to be used. The simplified PAB is filled with air before the inflator is triggered. Hence, a different mass flow curve had to used in order to compensate for all the air that is initially in the bag. It is therefore likely that the presented method to simplify a PAB will never imitate the more detailed PAB which is going from a folded state to unfolded. However, the behavior of the KNAB and its interaction with the dummy are much more simple. Therefore. it is much more suitable for simplification as an unfolded bag.

Further, the pressure curves between the simplified and detailed airbags never became the same even after the parameter tuning. Thus, another way to define the pressure may be used. Other studies have been using simpler computer models of the airbags where only the pressure within the bag is defined. However, using these models would erase the possibility to use the inflator or ventilation hole as varying parameters the same way they are defined today. A possible solution for future projects may be to parameterize a pressure curve such that a change in ventilation hole diameter is connected to the parameterize pressure curve. For instance, if the ventilation hole is increased by $P_1\%$, the average pressure goes down $P_2\%$. Although, the proposed solution must be studied further.

The simplified model deviated from the reference in general in terms of both risk injury criteria and kinematics. However, it is possible that trends can still be visualized, for example if the HIC value is increased from 850 to 900 when changing a parameter in the simplified model, it would most likely increased in the reference model as well, but it is not possible to say that it will be 900. An internal study done by VCC showed similar trends between HIC and chest deflection values compared to VPI. However, Only a few simulations were performed and the results should be handled with caution. Further studies are needed to say that all trends in the simplified model are applicable in more detailed models.

5.4 Stochastic simulation

The main result of the project ends with the stochastic simulation and the correlation analysis between the parameters. The most obvious finding to emerge from the analysis is that the pulse influences the system output more than all the other inputs, i.e. a higher VPI results in higher values of the risk indicators and a difference in dummy kinematics. As mention above, these relationships may partly be explained by the fact that the VPI is computed as a sort of risk criteria itself and is therefore closely related to these. However, according to these data, one can infer that a low VPI is something to aim for and it is a simple expression to evaluate the pulse in the design phase of a car project. Another interesting finding was that the injury criteria has a negative correlation against the length of the PAB, i.e. a longer PAB resulted in lower injury criteria. One possible explanation for this is that the dummy is slowed down during a longer distance which should lead to a lower acceleration peak. Hence, the dummy has not started to rotate forward when the contact between PAB and dummy occurs which will lead to most of the force goes through the chest. In short, the results indicates that the stochastic simulation can be a valuable tool for dimension of the safety system.

Further, the kinematics correlated with the risk indicators, e.g. the angle between the femur and the chest and the chest clip 3ms acceleration. The result show that if the chest is tilted more forward, the acceleration of the chest is higher. Although, it could be argued that the strong correlation between the rotation angles and the risk indicators is due to the strong influence of the pulse. As mention above, the VPI correlates with the risk criteria, but it is also well correlated to the kinematics. Therefore, a note of caution is due here since it may be that the kinematics and risk indicators would not correlate to to each other if the pulse was held constant.

The stochastic simulations also showed a wide spread of the risk indicator values. This finding is interesting as it supports the background and need for this project. Today, most simulations are performed with nominal values with no variation involved. However, the stochastic simulations showed that changing five input parameters led to a large spread of the risk indicators, e.g. the HIC36 vary from 440 to 890 or the CCLIP3m from 40 to 65 g. Spread is also found in physical crash tests, see e.g. Saunders and Parent [3]. Therefore, stochastic simulations should be included in the design process of a car project to understand how to optimize the safety system and make it more robust.

It is important to bear in mind that the results and conclusions are only valid in the defined parameter range. For instance, increasing the diameter of the ventilation hole will not ensure that the HIC values continue to decrease. There will be a point where the diameter is so big that the pressure in the bag gets to low and the dummy will strike trough and hit the rigid surface behind the bag. Thus, the HIC values will start to increase. It is a chance that the picked parameter range was too narrow to capture correlations. For this reason, a wider range of the distributions should be defined if the aim is to get more reliable results from the correlation analysis.

The findings from correlation analysis are limited by the fact that only a linear correlation matrix was used. It can still exist correlation between parameters that is not linear, but quadratic or exponential. Hence, a note of caution is due if the matrix shows no correlation. The linear correlation was used as a first test of the method. Other methods can be included in the post-processing in further analysis.

Furthermore, the data from the stochastic simulation must also be interpreted with caution because it is performed with the simplified model. The simplified model is a simplification of a FE model, which in itself is not hundred percent accurate compared to physical test. Hence, conclusions on how well the results are reflected in reality must be taken with care. Besides, the project was limited in one load case only and a correlation between an output parameter and an input parameter may not hold for other load cases, e.g. rear impact.

6 | Conclusion

In this project the applicability of a stochastic approach for vehicle interior simulations in frontal impacts has been studied and it can be concluded that this approach is a step in the right direction to get a better understanding of the passenger restraint system.

Parameters affecting the frontal passenger in full frontal impacts have been defined and sorted into three different types, *production*, *design* and *real life*. The sorting was used as a tool to decide on which parameter distribution to use for the different parameters.

Crash pulse distributions have been defined by using the Vehicle Pulse Index and 28 generic pulse shapes with constant delta velocity have been re-scaled to fit the load case used in this thesis.

A way to measure the influence of varying input parameters in terms of kinematics of a virtual crash test dummy has been developed specially adapted for full frontal impacts.

Further, a simplified parameterized frontal passenger vehicle model has been created. Passenger airbag and knee airbag have been simplified as unfolded airbags and a method to tune the simplified bags to act like a detailed reference model has been presented with help of a parameterized gas inflator. A curve fitting function that measured the root mean square error between the reference airbag pressure and the simplified airbags was used to tune the mass flow for the simplified airbags. The floor and the windscreen have been modeled as rigid surfaces. Further, a detailed FE model of a Volvo car front seat has been simplified without loosing functionality in frontal impacts. It was found that the backrest had little effect and most of the parts could be removed together with several pretensioned bolt connections. The final simplified model has been validated against a FE model of a current Volvo car platform. With the current status, the run-time has been decreased from 8 hours to 35 minutes for a 150 milliseconds long simulation with 240 cores. The shape of the simplified PAB was shown to deviate to much from the reference and the validation indicates that the exact numbers given from the simplified model cannot be directly compared to the reference model, for example values of the risk injury criteria, which is a limitation in this thesis.

The possibility to run stochastic simulations with LS-OPT at the CAE group at Occupant safety has been introduced. Further, stochastic simulations have been performed with geometrical, impact and airbag parameters varied. The statistical information such as mean, standard deviation and correlation between parameters has been evaluated. Moreover, different ways to present the data, i.e. scatter plots and history curves based on time data have been shown. The stochastic simulations indicated that a crash pulse with low VPI is to strive for when developing a car to get low values of the risk indicators in full frontal impact. It was also seen that the pulse shape has a large influence of the outcome of the frontal impact and it influences the system more than the other parameters varied in the passenger airbag. Hence, more clear relationships between airbag parameters and output parameters could bee seen if the pulse was varied less.

In short, the whole procedure from parameter selection, model development and validation and stochastic simulations have been developed and described. Both the gain of the method and its limitations have been mentioned and some options to overcome these constraints have been presented.

7 | Further Investigations

After the initial development of the methodology implemented in this project, further investigations and model development might be performed in order to improve the model quality, statistical information of input parameters and the results.

In the future, more statistical information must be gathered in the car projects in order to implement stochastic simulations into the design process, e.g. real data from manufacturing. Further, real life parameters from data bases can be gathered in order to ensure a more robust system in "real life" crashes.

Further work needs to be done to establish which parameters are most relevant to vary in the simulations, e.g. a Design of Experiment could be performed. The aim is to see which one of the input parameters influences the system the most. The result can be used to rate the parameters from highest impact to lowest. In order to keep the number of simulations small, only the top 5 to 10 parameters would be used in stochastic simulations.

Furthermore, the model could be extended for more load cases, e.g. frontal overlap impacts. Hence, including a belt, door panel and curtain airbag. As long as there are tests that the model can be validated against, a more generic setup can be achieved. However, adding more load cases leads to more possible input parameters which statistical information must be gathered.

Regarding model validation, considerably more work will need to be done to correlate the model further and make it an effective and trustworthy tool. The current level of the errors compared to the reference model are too large. Other ways to simplify the airbags or the floor must be evaluated, e.g. implementing springs connected to the rigid floor, making it possible to tune how stiff the impact between the floor and dummies feet should be. For the airbags, a defined bag pressure may be the way to go or to fold the simplified bags. In addition, a more detailed model of the dummy, for example the detailed Hybrid III 50th or THOR dummy which are better correlated.

It is also important to highlight the need for further validation between the simplified model and the reference model regarding varying parameters. The current model is validated against nominal values. No validation has been done to see if the change in parameters in the simplified model results in the same type of change in the more detailed reference model. For this, several tests must be performed.

A further study could assess the effects of number of simulations in the stochastic analysis. 150 simulations were performed in this thesis which was assumed to be enough. The influence of performing both less and more simulations would be interesting to study.

Finally, the processing of all the data from the stochastic simulation can be developed further. First, a quadratic correlation analysis can be included to not only see linear trends. Secondly, in order to speed up the processes, the post processing could be more automated with better scripts.

Bibliography

[1] Global status report on road safety 2018: summary, Geneva: World Health Organization; 2018 (WHO/NMH/NVI/18.20), Licence: CC BY-NC-SA 3.0 IGO.

[2] "Fatality Facts 2017," *Insurance Institute for Highway Safety*, Dec. 2018. `https://www.iihs.org/topics/fatality-statistics/detail/yearly-snapshot`, Accessed: 2019-05-28.

[3] J. Saunders and D. Parent, "Repeatability of a Small Overlap and an Oblique Moving Deformable Barrier Test Procedure," *SAE Int. J. Trans. Safety*, Volume 1, Page 309-327, Jul. 2013.

[4] R. Kent, J. Patrie and N. Benson, "The Hybrid III dummy as a discriminator of injurious and non-injurious restraint loading," in *Annual Proceedings/Association for the Advancement of Automotive Medicine,* Sep. 2003.

[5] J. Iraeus, "Stochastic Finite Element Simulations of Real Life Frontal Crashes," Ph.D. dissertation, Dep. of Surgical and Perioperative Sciences, Umeå University, Sweden, 2015.

[6] X. Deng, S. Potula, H. Grewal, K.N. Solanki, M.A. Tschopp and M.F. Horstemeyer, "Finite element analysis of occupant head injuries: Parametric effects of the side curtain airbag deployment interaction with a dummy head in a side impact crash," *Accident Analysis Prevention*, Volume 55, Page 232-241, Jun. 2013.

[7] *Road vehicles – Traffic accident analysis – Part 3: Guidelines for the interpretation of recorded crash pulse data to determine impact severity,* ISO/TR 12353-3:2013, Jan. 2013.

[8] J. Will and H. Baldauf, "Integration of Computational Robustness Evaluations in Virtual Dimensioning of Passive Passenger Safety at the BMW AG," *Numerical Analysis and Simulation in Vehicle Engineering*, VDI Report Nr. 1976, Page 851-873, 2006.

[9] K. Taewung, and J. Hyun-Yong, (2010). "Stochastic analysis of the variation in injury numbers of automobile frontal crash tests," *International Journal of Automotive Technology*, Volume 11, Page 481-488, Aug. 2010.

[10] M. Avalle, G. Belingardi, A. Ibba, K. Kayvantash, F. Delcroix, "Stochastic crash analysis of vehicle models for sensitivity analysis and optimization," in *20th ESV conference*, Lyon, France, Jun. 2007.

[11] K. Dongseok, L. Mansu, K. Jeasu, H. Jaenyung, P, Jaewon and Y. Sangha, "A Study of Dummy Kinematic and Restraint System for IIHS Small Overlap Frontal," in *23rd International Technical Conference on the Enhanced Safety of Vehicles (ESV)*, Seoul, South Korea, 2013.

[12] C. Bastien et al., "Influence of human bracing reflex on occupant's neck, head and thorax injuries in emergency braking combined with an FMVSS208 impact scenario," in *ICrash*, Milan, 2012.

[13] H. Mertz and A. Irwin, "Anthropomorphic Test Devices and Injury Risk Assessments," in Accidental Injury: Biomechanics and Prevention, Yoganandan et al., New York, NY: Springer New York, 2015, ch. 4, Page 83-112.

[14] "Hybrid III 50th Male," *Humanetics*, 2019. URL: `http://www.humaneticsatd.com/crash-test-dummies/frontal-impact/hiii-50m`, Accessed: 2019-02-04.

[15] "THOR 50th Male," *Humanetics*, 2019. URL: `https://www.humaneticsatd.com/crash-test-dummies/frontal-impact/thor-50m`, Accessed: 2019-05-14.

[16] *Orientations of standardized dummy coordinate system for standing and seated postures,* SAE J211, Oct. 1994.

[17] "The New Car Assessment Program Suggested Approaches for Future Program Enhancements," *National Highway Traffic Safety Administration*, 2007. URL: `https://www.safercar.gov/staticfiles/safercar/pdf/810698.pdf`, Accessed: 2019-05-14.

[18] Occupant Crash Protection, FMVSS208, Jan. 2014.

[19] K. Digges, "Injury Measurements and Criteria," presented in the 'RTO HFM Specialists' Meeting on "Models for Aircrew Safety Assessment: Uses, Limitations and Requirements", Ohio, USA, Oct. 1998. [Online] Available: `https://apps.dtic.mil/dtic/tr/fulltext/u2/a368371.pdf#page=177`.

[20] R. Eppinger, et al., "Development of Improved Injury Criteria for the Assessment of Advanced Automotive Restraint Systems - II," *Association for the Advancement of Automotive Medicine*, NHTSA, Tech. rep., 1999.

[21] *LSTC Hybrid III 50th Fast Dummy*, Version 2.0, Livermore Software Technology, Michigan, 2011.

[22] F. Yang and M. Beadle, "CAE Analysis of Passenger Airbag Bursting through Instrumental Panel Based on Corpuscular Particle Method," in *10th European LS-DYNA Conference*, Würzburg, Germany, 2015.

[23] A. Hirth, A. Haufe and L. Olovsson, "Airbag simulation with LS-DYNA, Past-Present-Future," in *6th German LS-DYNA forum*, Frankenthal, Germany, 2007.

[24] *LS-DYNA Keyword User's Manual Volume I,* Version R9.0 revision 7883, Livermore Software Technology Corporation, California, Aug. 2016.

[25] N. M. Lafontaine, R. Rossi, M. Cervera and M. Chiumenti, "Explicit mixed strain-displacement finite element for dynamic geometrically non-linear solid mechanics," in *Computational Mechanics*, Volume 55, Page 1-17, Mar. 2015.

[26] S. Mattern, C. Schmied and K. Schweizerhof, "Highly efficient solid and solid-shell finite elements with mixed strain–displacement assumptions specifically set up for explicit dynamic simulations using symbolic programming," *Computers & Structures*, Volume 154, Pages 210-225, Jul. 2015.

[27] *LS-OPT User's Manual,* Version 5.1, Livermore Software Technology Corporation, California, Jun. 2014.

[28] *Ansa User's Guide,* Version 19.1.x, BETA CAE Systems, Switzerland, Oct. 2018.

[29] *META Post Processor User's Guide,* Version 19.0.x, BETA CAE Systems, Switzerland, Oct. 2018.

[30] J. Iraeus, M. Lindquist, S. Wistrand, E. Sibgård and B. Pipkorn, "Evaluation of Chest Injury Mechanisms in Nearside Oblique Frontal Impacts," *Annals of advances in automotive medicine*, vol 57, Page 183-196, Sep. 2013.

[31] J. Will, C. Bucher. "Statistical Measures for the CAE - based Robustness Evaluation," *Proceedings Weimarer Optimierungs- und Stochastik tage 3.0*, Weimar, Germany, 2006.

A | Detailed data of the generic pulses

Detailed data of the 28 pulses used as input parameters to the stochastic simulation is shown in Table A.1. Moreover, the statistical distribution of the VPI from the 28 pulses are presented in a histogram in Figure A.1. Lastly, examples of 6 pulse shapes are plotted against both time and stopping distance in Figure A.2.

Table A.1: Data from the 28 pulses used as input parameter for stochastic simulations.

ID	VPI [g]	Stopping distance [mm]	Delta velocity [mph]	Stop time [ms]
1	38.9	395	28.2	83
2	40.4	496	28.5	83
3	41.9	440	28	83
4	45.8	393	28.6	83
5	41.7	439	28.8	83
6	39.4	428	28.6	86
7	40.2	490	28.6	86
8	42.9	501	28.7	86
9	37.3	449	28.2	86
10	40.8	458	29.1	89
11	40.7	458	29.1	83
12	39.2	456	28.6	83
13	38.8	451	28.6	83
14	38.1	447	28.5	86
15	41.5	451	28.6	83
16	38.9	451	28.6	87
17	37.6	444	28.4	87
18	42.9	456	28.8	87
19	42	450	28.5	87
20	43.9	457	28.8	80
21	43.8	449	28.7	80
22	41.6	443	28.6	84
23	45	445	28.9	80
24	40.8	443	28.4	83
25	39.6	456	28.7	89
26	41.9	446	28.8	83
27	40.5	463	28.3	89
28	40.3	440	28.4	86

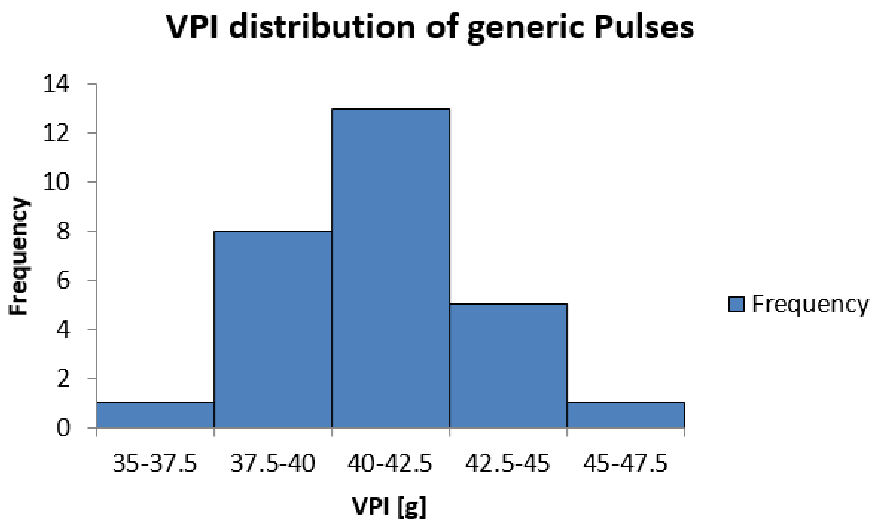

Figure A.1: Histogram of VPI distribution of 28 generic pulses, $\mu = 40.9$, $\sigma = 0.404$.

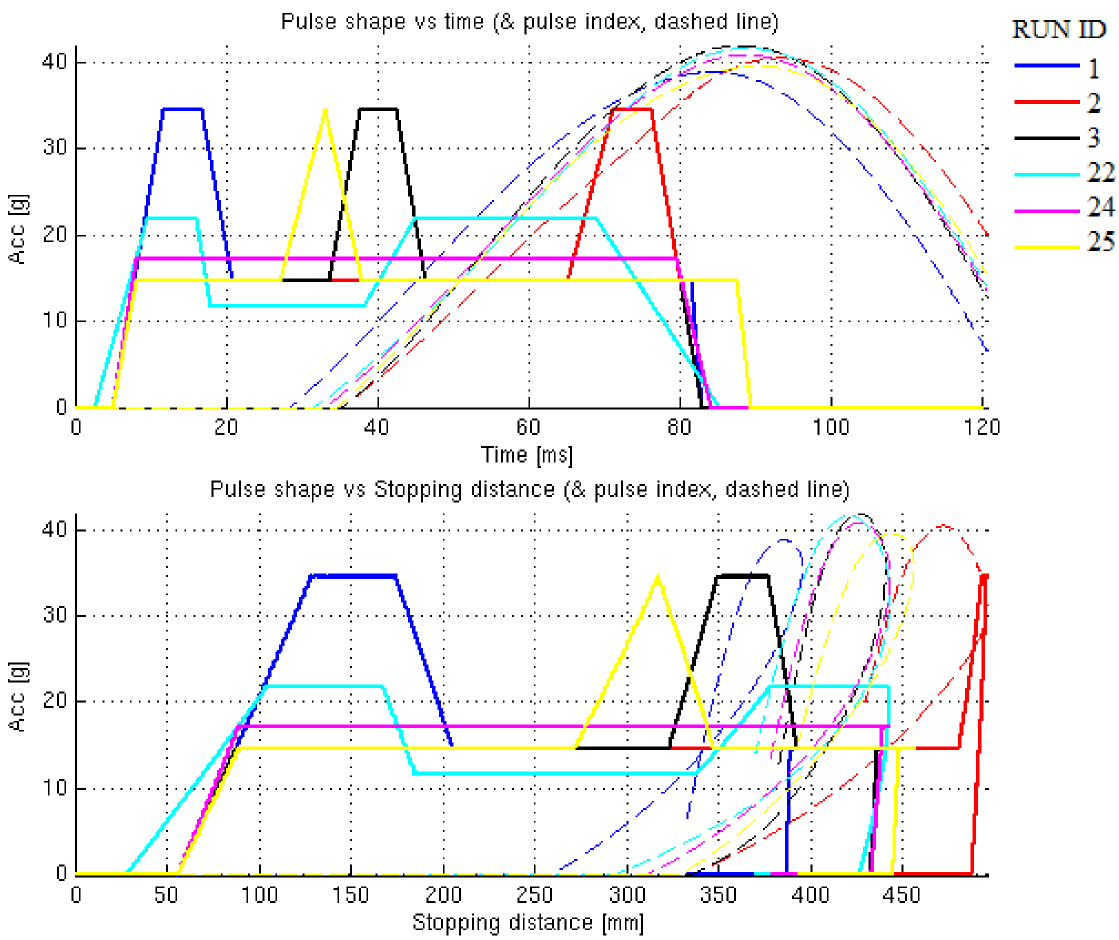

Figure A.2: Examples of pulse shapes and VPI plotted versus time and stopping distance. Pulse ID shown is 1, 2, 3, 22, 24 and 25.

B | Injury critera values from one to one testing

A more detailed comparison from the one to one tests between the reference model and the seat, PAB, tuned PAB, KNAB and tuned are presented in Table B.1. The comparison with the FAST50 dummy is not included since it not possible to extract all the data from that model. Moreover, the table compares measures all the way from the head down to the knee.

Table B.1: Risk indicators comparing the output from the one to one comparison of the seat, PAB and KNAB.

Measure	Max/Min	Units	Reference	Seat	PAB	PAB - Tuned	KNAB	KNAB - Tuned
HIC36	Max	-	532	498	976	1020	694	615
HIC15	Max	-	425	380	849	880	491	460
Head Acceleration Res.	Max	g	66.6	61.6	103	89.6	71.2	68.8
Head Acceleration Res. Clip3ms	Max	g	65.2	61.1	85.3	88.5	70	67.4
Head Acceleration X	Abs(Min)	g	65.9	59.7	101	88.6	70.7	68.3
Head Acceleration Y	Abs(Min)	g	9.89	18.2	11.6	8.63	9.02	9.25
Head Acceleration Z	Max	g	23.4	57.4	62.7	44.1	55.5	62.3
Upper Neck Fx	Max	kN	1.7	1.39	2.69	2.84	1.42	1.47
Upper Neck Fz	Max	kN	0.885	1.82	1.52	1.32	1.6	2.39
Upper Neck Fz -	Abs(Min)	kN	-0.732	-1.6	-1.93	-1.2	-1.62	-2.15
Upper Neck My -	Abs(Min)	Nm	-22.2	-24	-22.2	-44	-36.2	-34.2
Lower Neck Fx	Max	kN	1.91	1.9	2.02	2.09	1.89	2.06
Lower Neck Fz	Max	kN	1.06	1.55	1.06	2.18	1.95	1.58
Lower Neck My	Abs(Min)	Nm	-202	-197	-194	-218	-223	-232
Upper Nij	Max	-	0.386	0.34	0.746	0.449	0.319	0.373
Lower Nij	Max	-	1.82	1.8	1.78	1.9	2.11	2.14
Thoracic Spine Fx	Abs(Min)	kN	1.49	1.37	1	2.34	1.78	1.85
Thoracic Spine Fz	Max	kN	3.31	3.33	1.81	5.08	5.99	5.35
Thoracic Spine My	Abs(Min)	Nm	194	188	297	325	249	247
Lumbar Spine Fz	Abs(Min)	kN	2.83	3.17	3.1	2.96	3.63	3.21
Lumbar Spine My	Max	Nm	401	382	202	543	483	484
Chest Res. Aceleration	Max	g	52.7	50.3	62.3	63	58.7	59.9
Chest Res. Acc. Clip3ms	Max	g	51.1	49.5	61.5	61.2	56.3	58.5
Chest X Aceleration	Abs(Min)	g	46.6	42.9	61.5	53.8	52.3	52.9
Chest Y Aceleration	Max	g	2.99	6.02	3.21	5.19	3.19	6.52
Chest Z Aceleration	Max	g	25.6	27.2	13	34.5	29.9	29.6
Chest Def.	Max	mm	18.6	16.4	38.9	13.1	20.5	20.1
hest Def. Rate	Max	mm/msec	0.971	1.06	2.62	1.2	0.929	0.977
Chest VC	Max	-	0.066	0.06	0.341	0.06	0.095	0.097
Pelvis Acceleration X	Abs(Min)	g	48.6	51.3	47.7	46.8	58.7	55
Pelvis Acceleration Y	Max	g	4.37	4.32	4.43	5.31	3.69	3.95
Pelvis Acceleration Z	Abs(Min)	g	24.3	22.2	17.1	29.9	34.3	30.3
Pelvis Acceleration Res.	Max	g	51.4	53.9	49.6	52	61.4	57.4
Left Femur Fz	Abs(Min)	kN	-5.99	-5.4	-5.61	-5.79	-6.35	-6.14
Right Femur Fz	Abs(Min)	kN	-3.96	-4.5	-4.53	-4.1	-6.49	-5.82
Knee Clevis Left Inner Fz	Abs(Min)	kN	3.24	2.85	3.08	3.34	2.98	3.1
Knee Clevis Left Outer Fz	Abs(Min)	kN	2.68	2.68	2.74	2.74	2.92	2.76
Knee Clevis Right Inner Fz	Abs(Min)	kN	2.76	2.98	3.14	2.8	3.29	3.25
Knee Sliders Left Disp.	Max	mm	7.58	9.52	6.34	7.28	11.1	10.3
Knee Sliders Right Disp.	Max	mm	8.99	8.09	6.25	7.35	11.9	13.3
Upper Left Tibia Index	Max	-	0.764	0.7	0.72	0.734	0.709	0.894
Upper Right Tibia Index	Max	-	0.857	0.7	0.787	0.737	0.643	0.873
Lower Left Tibia Index	Max	-	0.786	0.55	0.844	0.936	0.691	0.792
Lower Right Tibia Index	Max	-	0.833	0.81	0.673	0.77	0.854	1.11